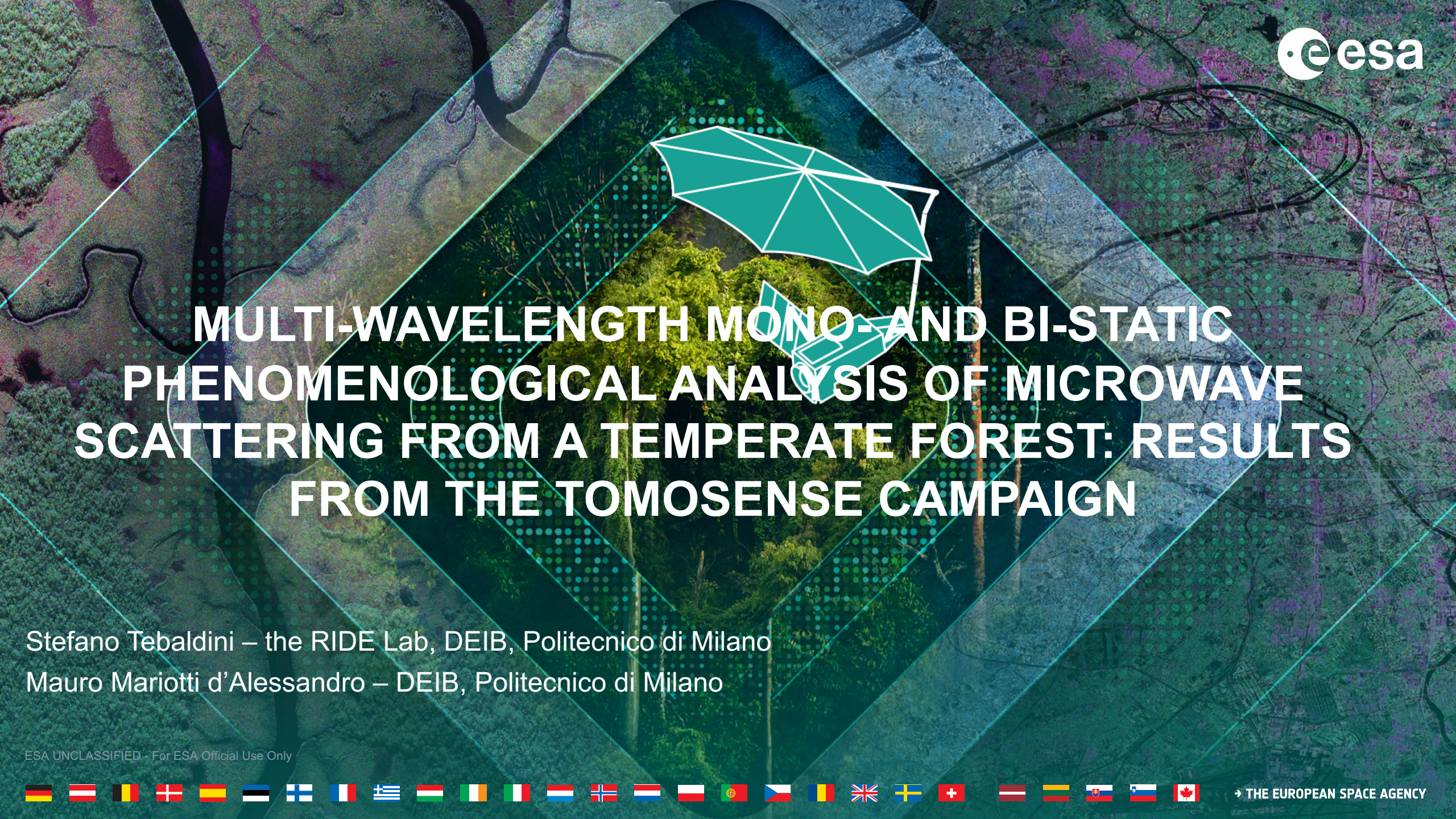

MULTI-WAVELENGTH MONO- AND BI-STATIC PHENOMENOLOGICAL ANALYSIS OF MICROWAVE SCATTERING FROM A TEMPERATE FOREST: RESULTS FROM THE TOMOSENSE CAMPAIGN

Stefano Tebaldini – the RIDE Lab, DEIB, Politecnico di Milano
Mauro Mariotti d'Alessandro – DEIB, Politecnico di Milano

TomoSense

TomoSense is an ESA campaign to support R & D of bistatic and tomographic Synthetic Aperture Radar (SAR) observation techniques for forest applications in support of future SAR mission concepts at P-, L-, and C-band.

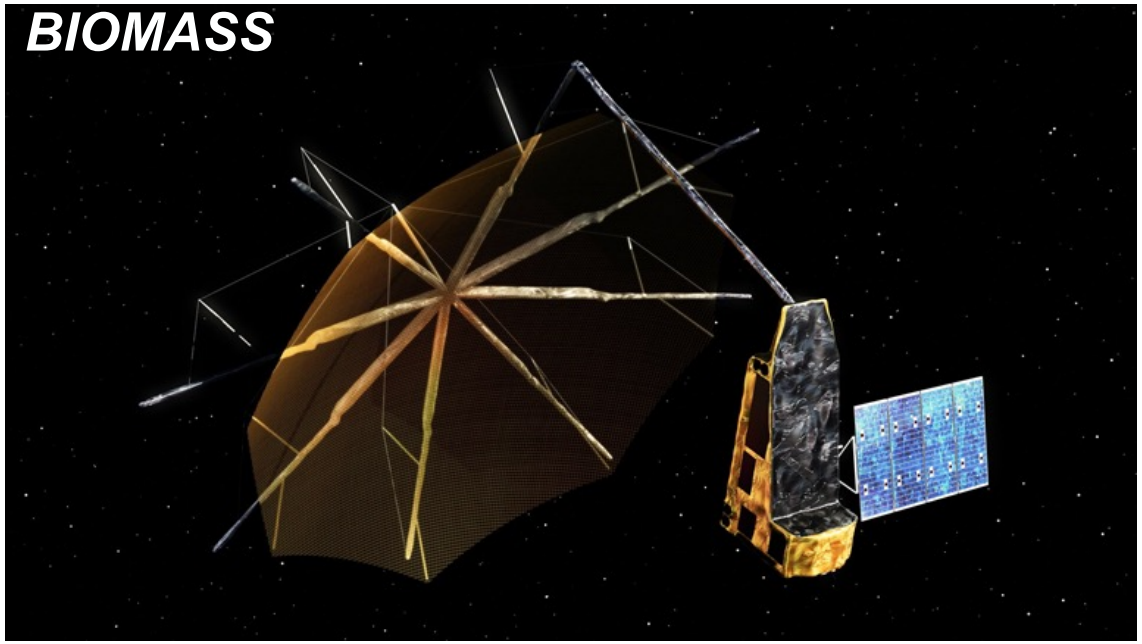

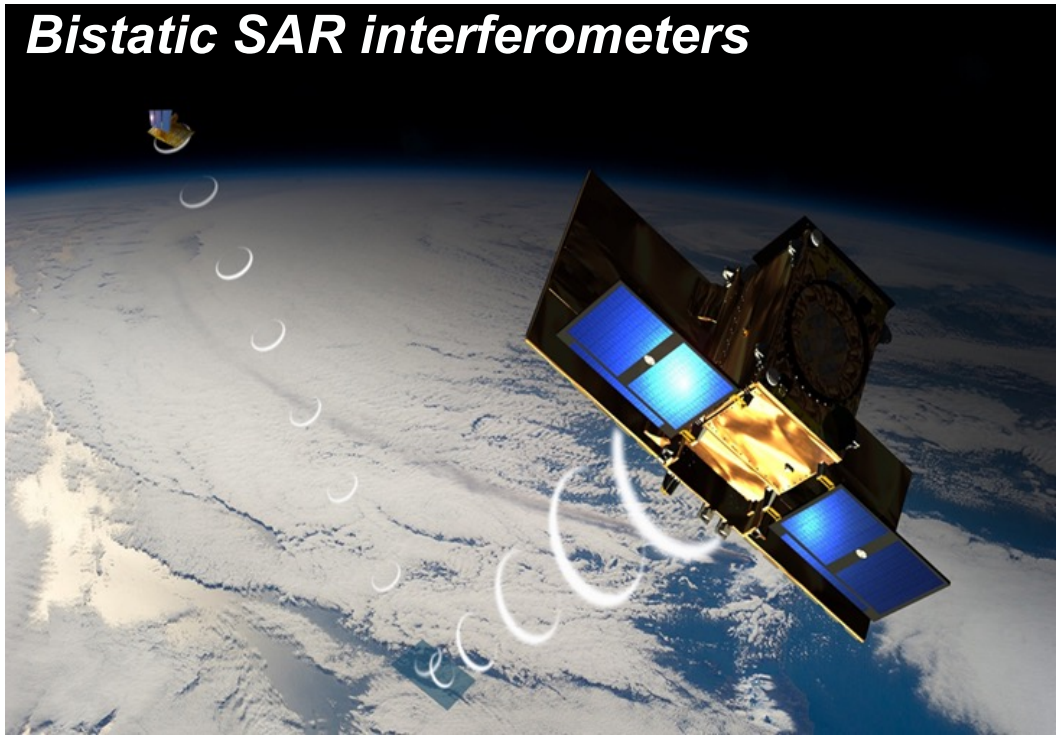

The TomoSense campaign

The airborne campaign took place in 2020/21 at the Kermeter site in the Eifel National Park in North-Rine Westphalia in Germany. The campaign includes:

- Bistatic airborne SAR surveys at L- and C-Band collected by flying two aircraft in close formation, with one following the other at a nominal distance of approximately 20/30 m.
- The flights were programmed in synergy with the P-Band campaign BelSAR-P.
- In-situ collection of relevant forest parameters at approximately 80 plots.
- Collection of TLS data at a scale of 1 ha at 10 plots.
- Installation of 5 m trihedral reflectors for P-Band calibration

Flight plan

SAR acquisitions at P-, L-, and C-Band are carried out by repeatedly flying the Radar sensors along an oval-like racetrack, so as to have around 20 or more passes from two opposite flight headings

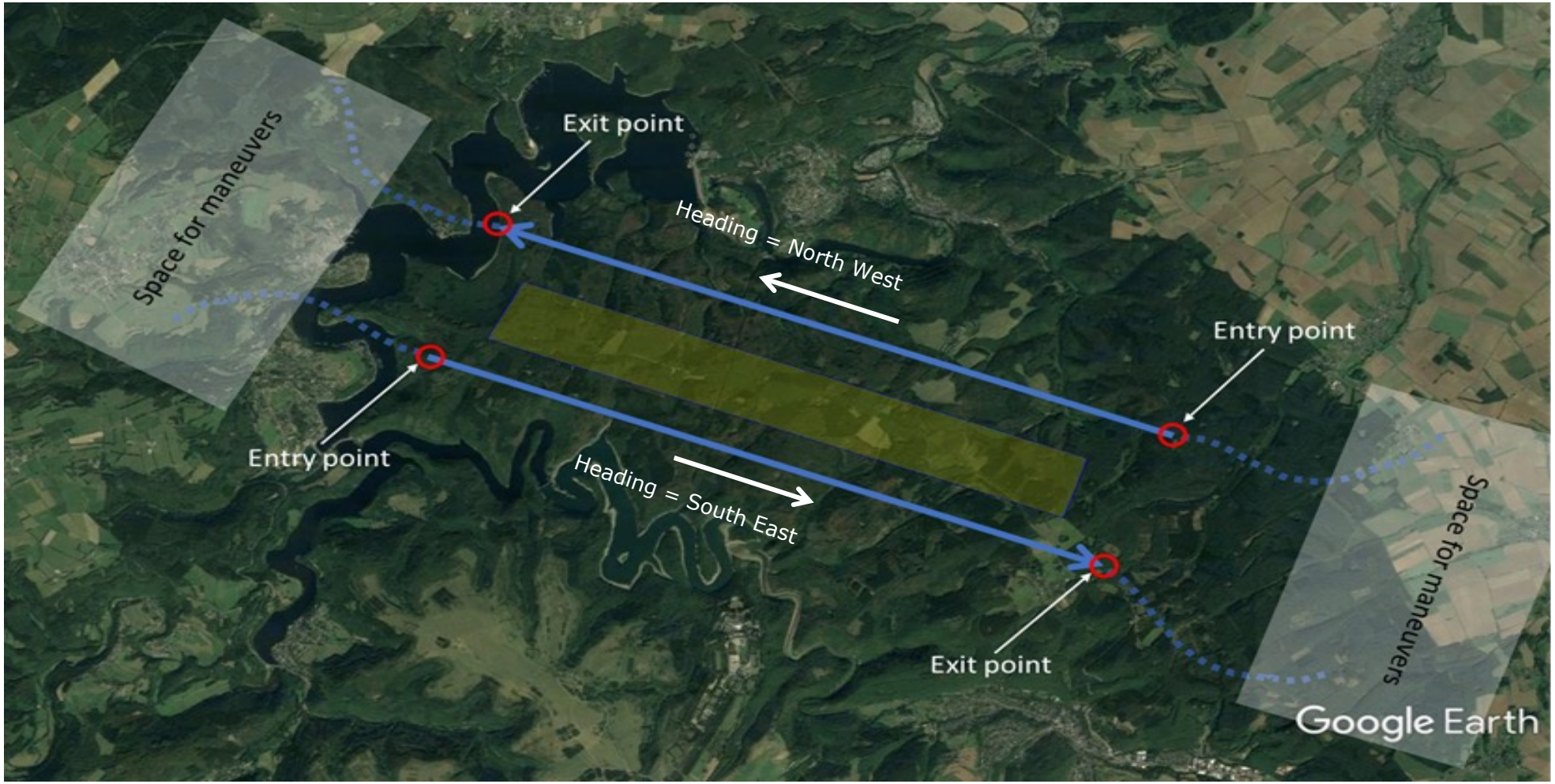

Flight plan – P-Band

Flight height variation in 20 passes (meters w.r.t. 2200 m)

0 0 0 0 0 0 0 0 0 0 -4 -8 -12 -16 -20 -24 -28 -32 -36 -40

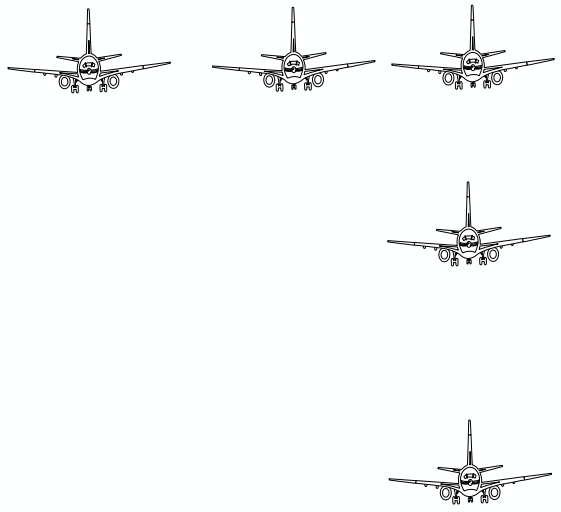

Fly 10 passes at the same height, then decrease flight height by 4 m every pass

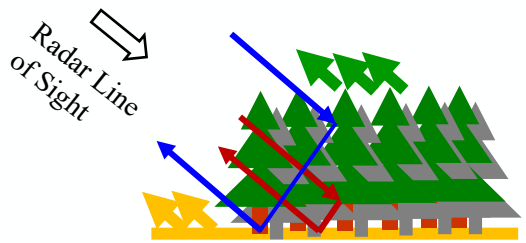

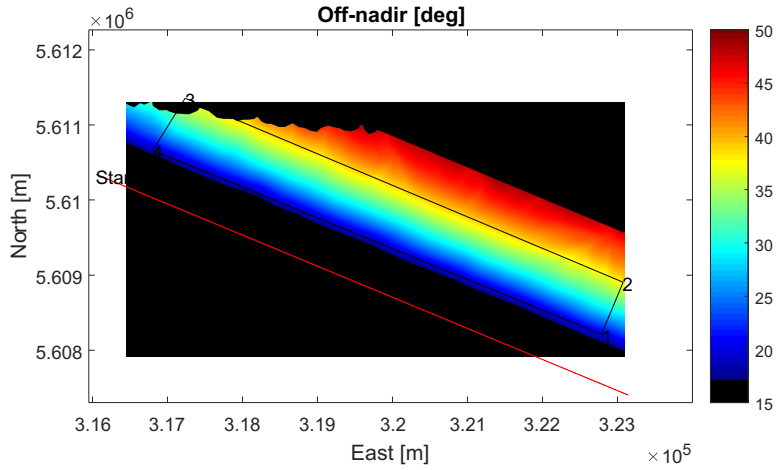

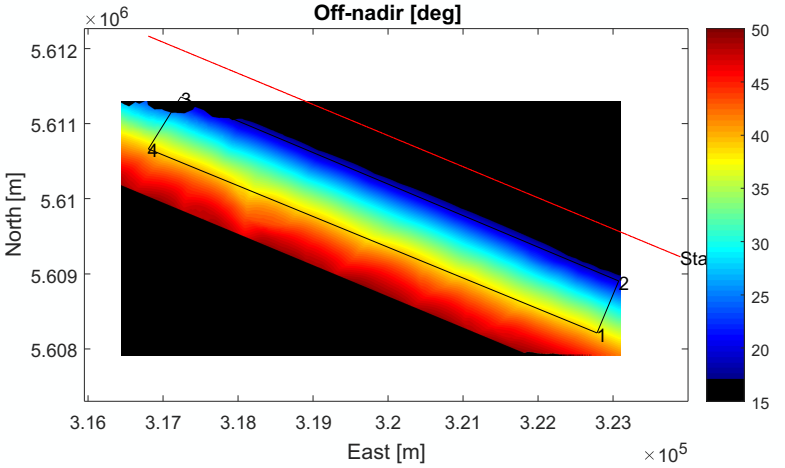

Flight plan – L-Band

Slave flights 30 m to the left w.r.t. Master (if Radar is left-looking)

Master flights ahead by 20/30 m (preferably 30 m)

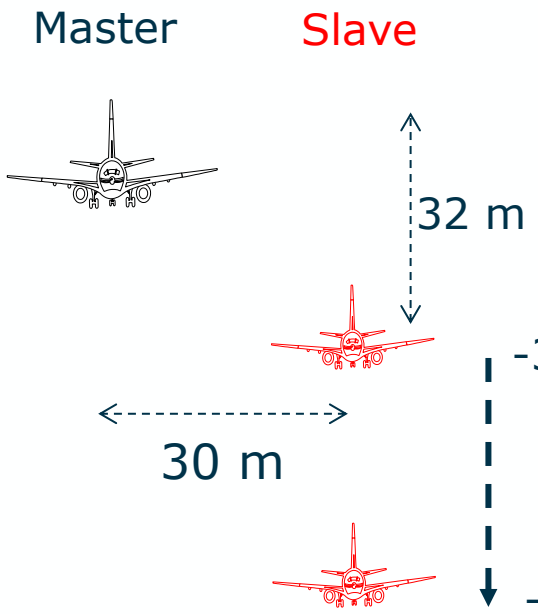

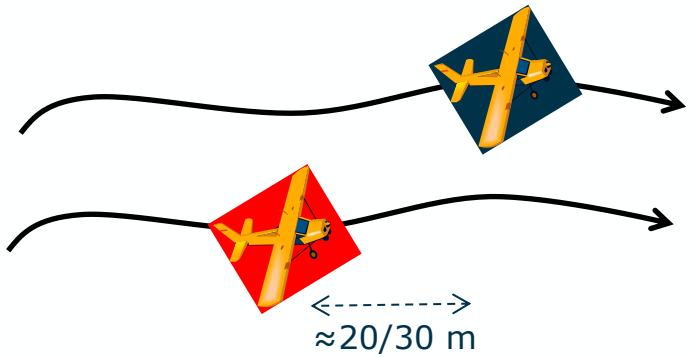

Slave starts 32 m lower than Master in the first flight

Then decreases flight height by 3 m every pass

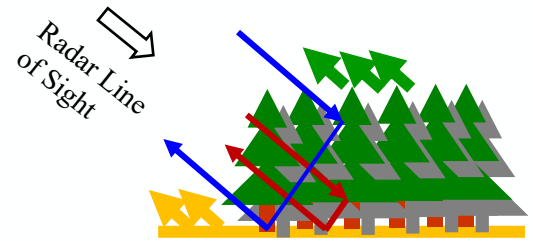

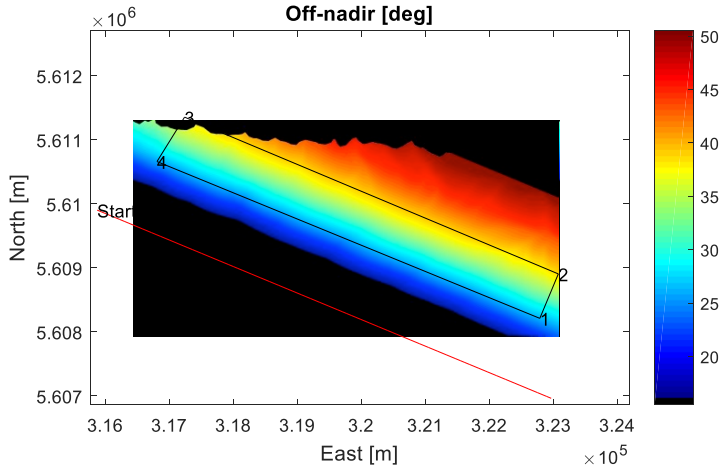

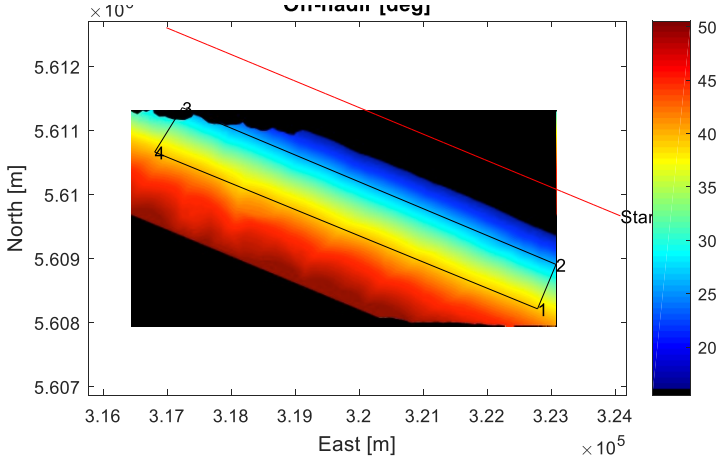

Flight plan – C-Band

Slave flights 20 m to the left w.r.t. Master (if Radar is left-looking)

Master flights ahead by 20/30 m (preferably 20 m)

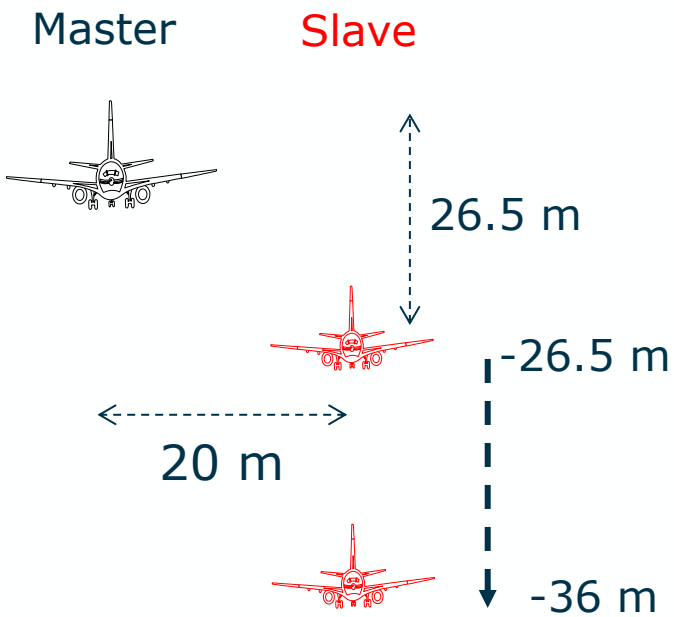

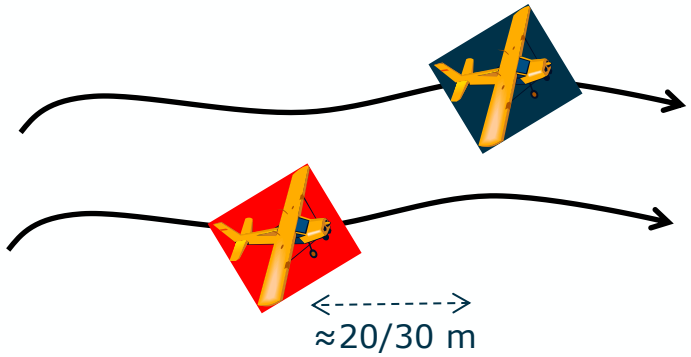

Slave starts 26.5 m lower than Master in the first flight

Then decreases flight height by 0.5 m every pass

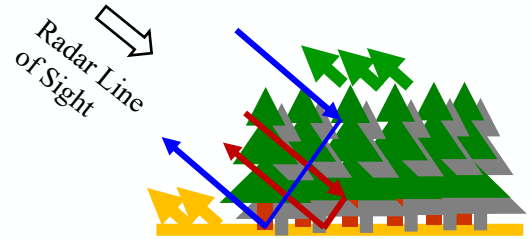

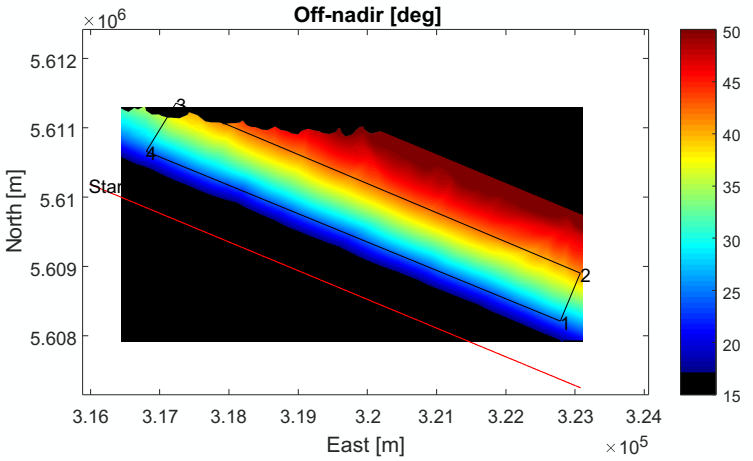

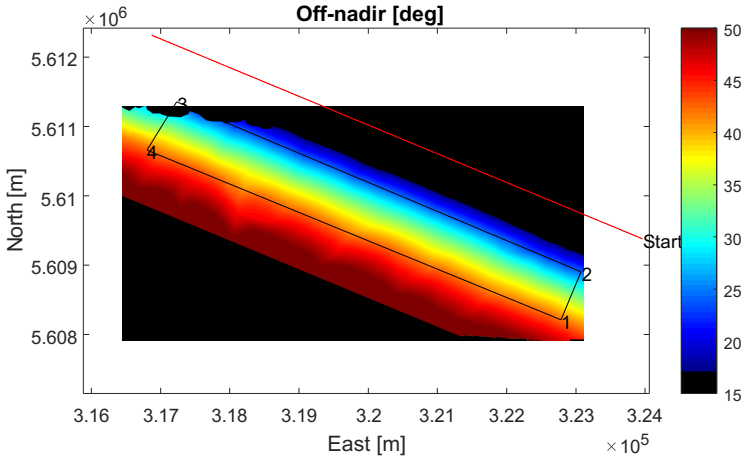

Campaign execution

Campaign execution took longer than expect due to several reasons:

- *delay in getting permission to transmit from local authority, a hardware glitch, bad weather (a storm capsized 5 m corner reflectors), global pandemics due to C19, the flood in North-West Germany in 2021…*
- The definition of bistatic baselines was misinterpreted in 2020 flights, preventing tomographic imaging. After discussion among ESA, PoliMi, and MS, it was decided to repeat C-Band flights in autumn 2021.

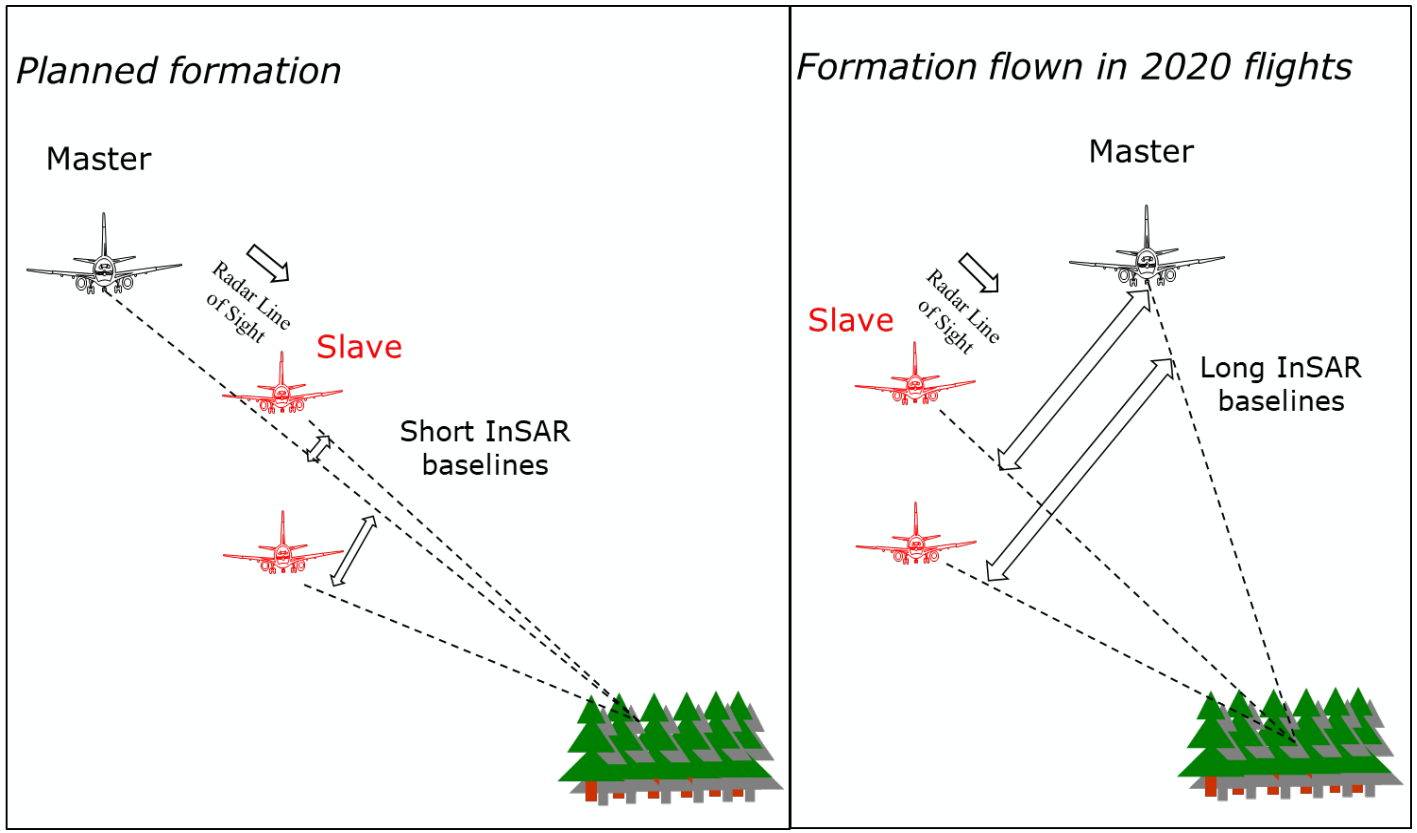

Tolerable at L-Band using dedicated tomographic processing

Show-stopper for C-Band

Interferometric calibration

The acquired data stack turned out to be affected by space-varying azimuth co-registration errors at large ranges due to residual baseline variations unpredicted by navigational data

⇒ ***Massive processing required***

Trajectory correction was carried out by Multi-Squint Interferometry

- Defocusing to raw data using trajectories from navigational data
- Formation of sub-images at different squint angles
- Trajectory estimation
- 2D Refocusing using corrected trajectories

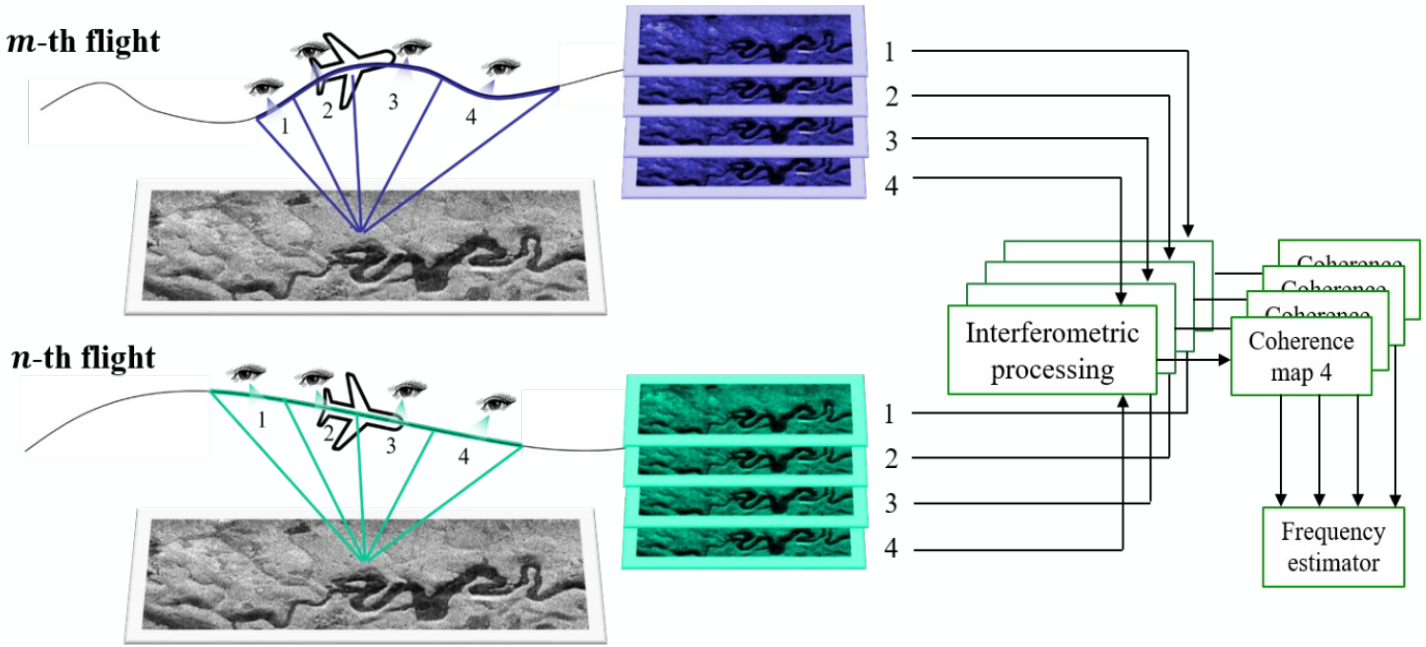

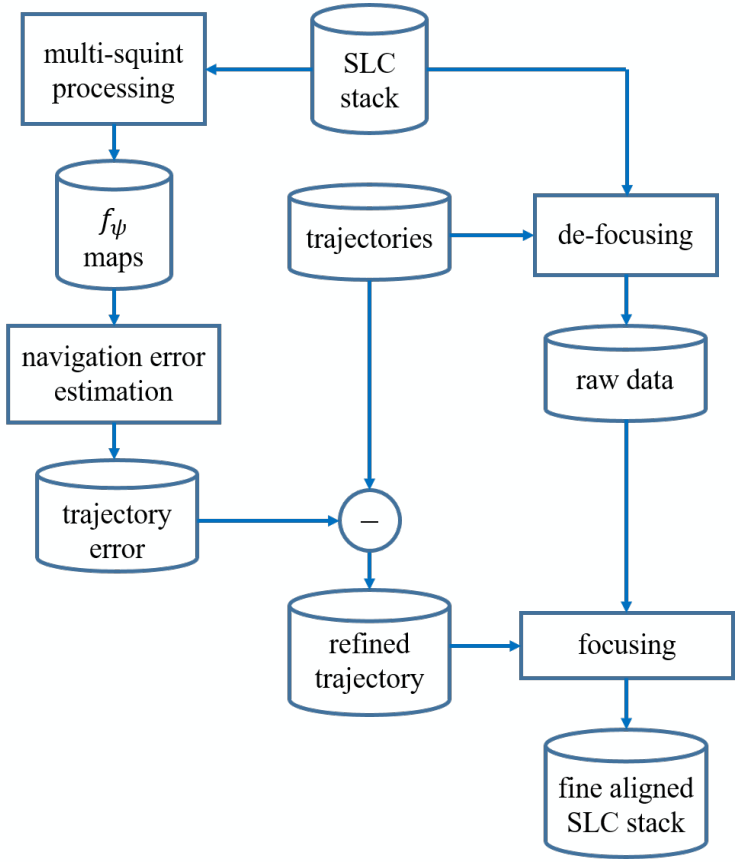

Thousands of interferograms processed

Interferometric calibration

The acquired data stack turned out to be affected by space-varying azimuth co-registration errors at large ranges due to residual baseline variations unpredicted by navigational data

⇒ ***Massive processing required***

Trajectory correction was carried out by Multi-Squint Interferometry

- Defocusing to raw data using trajectories from navigational data
- Formation of sub-images at different squint angles
- Trajectory estimation
- 2D Refocusing using corrected trajectories

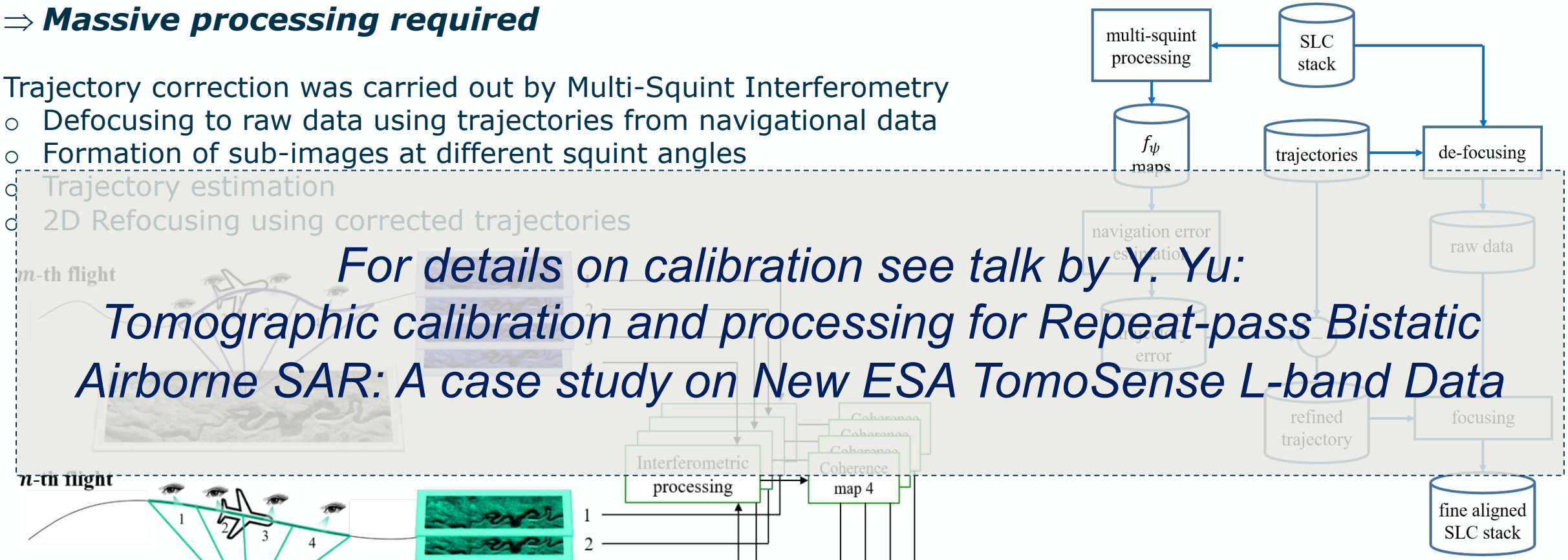

For details on calibration see talk by Y. Yu:
Tomographic calibration and processing for Repeat-pass Bistatic Airborne SAR: A case study on New ESA TomoSense L-band Data

Thousands of interferograms processed

P-Band Tomography

P-Band vertical section

- Repeat-pass
- Mono-static

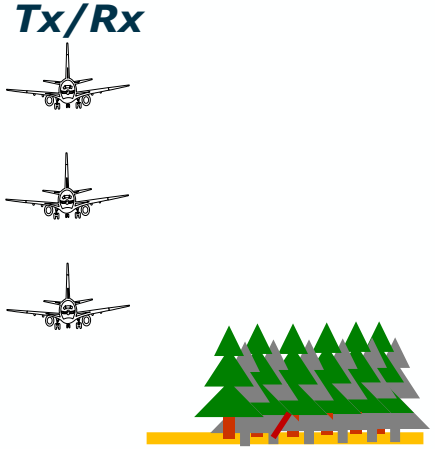

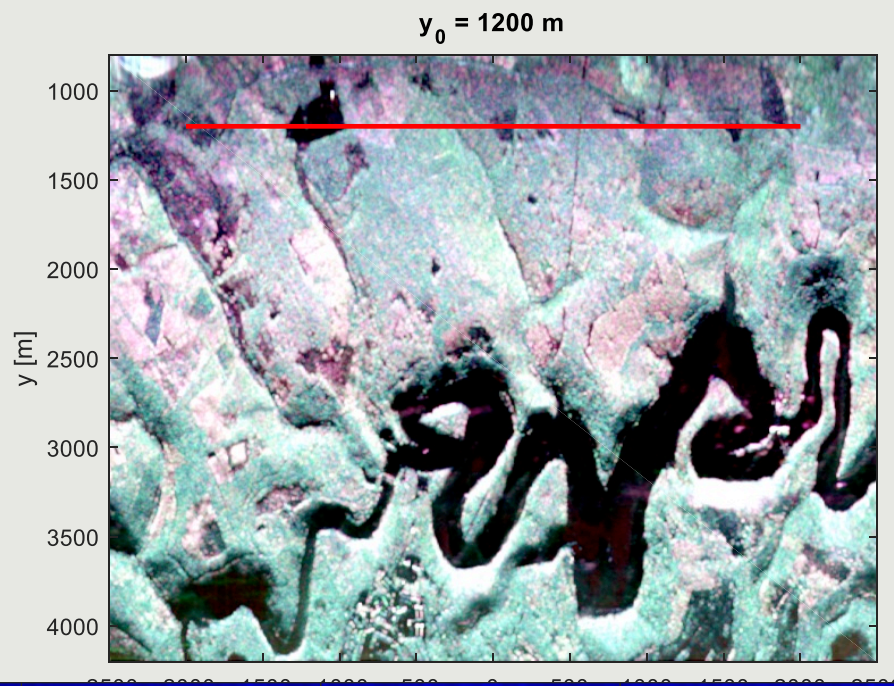

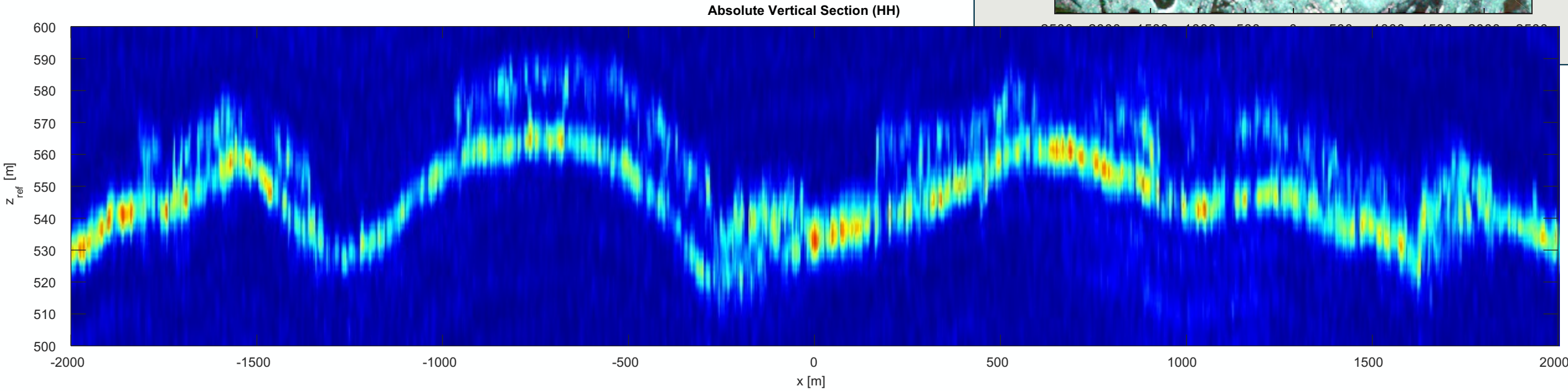

P-Band Tomography

P-Band vertical section

- Repeat-pass
- Mono-static

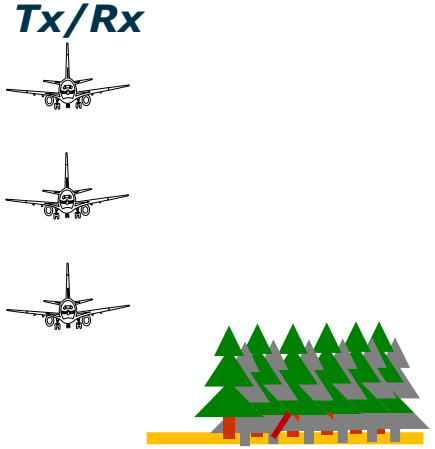

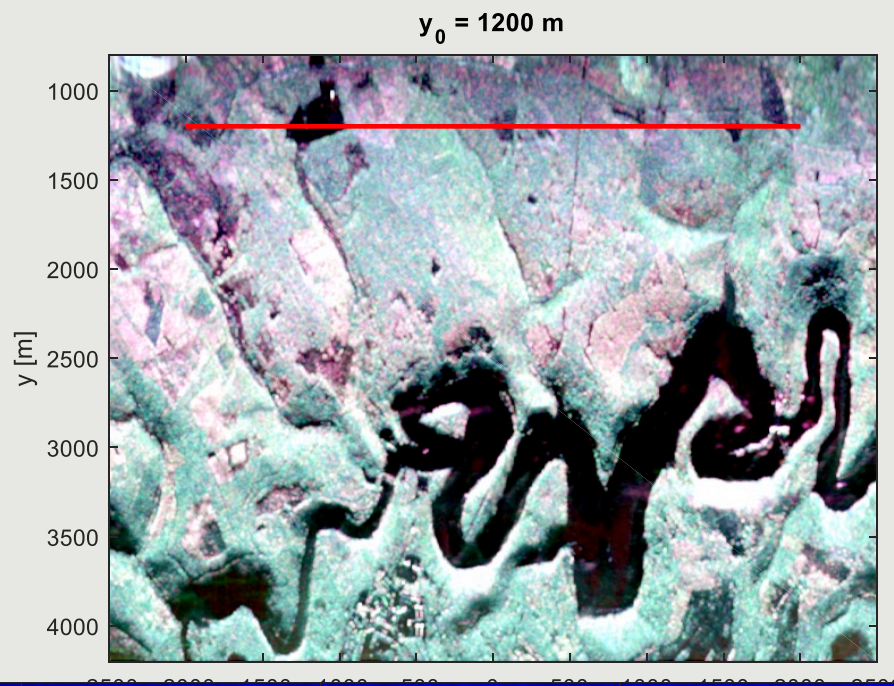

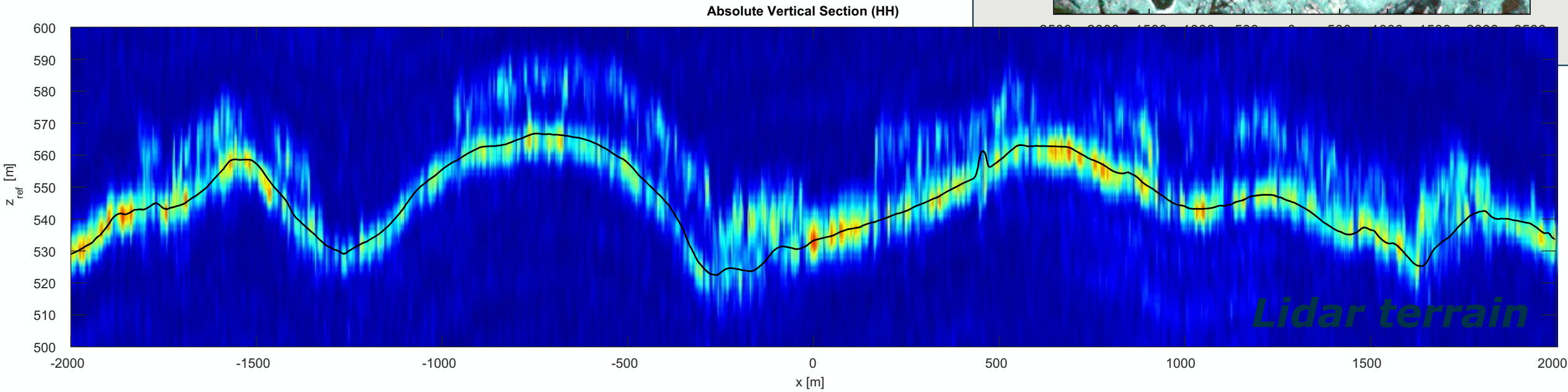

P-Band Tomography

Ground-steered P-Band vertical sections

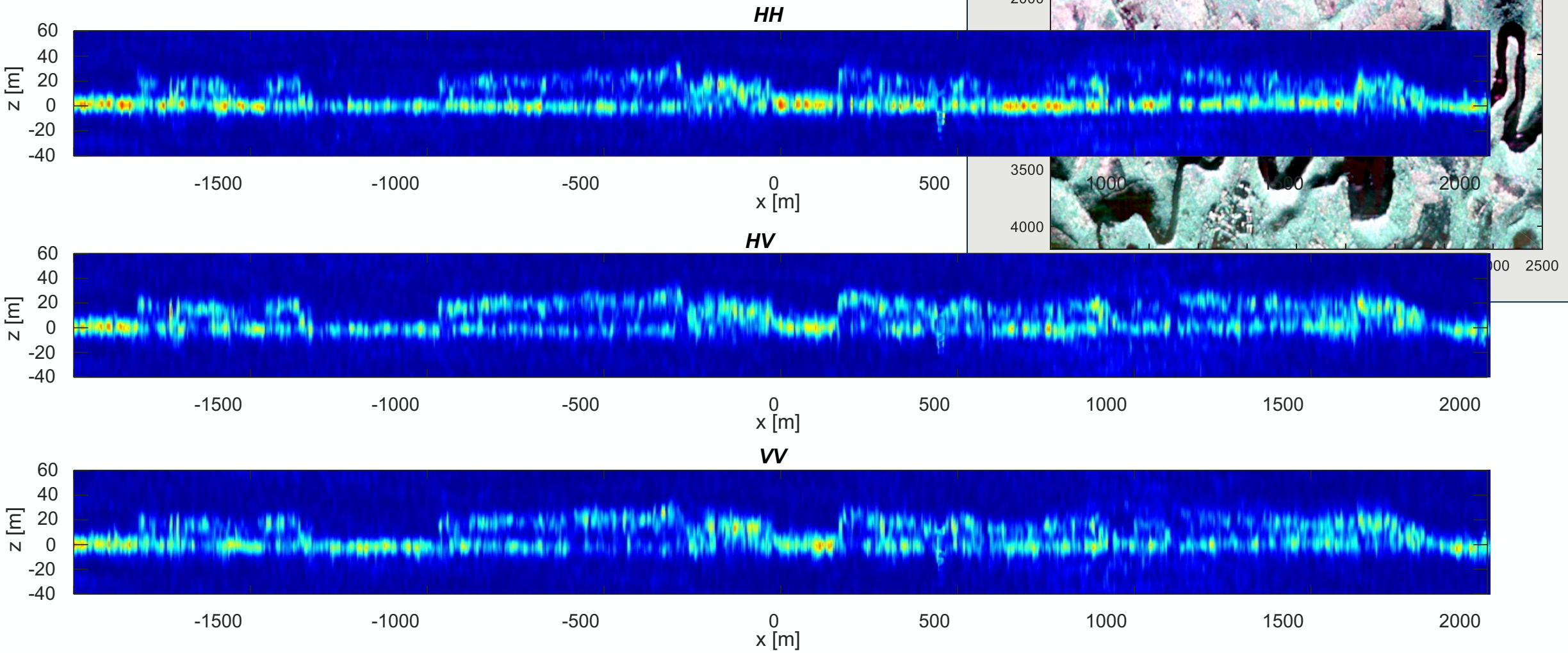

P-Band Tomography

Ground-steered P-Band vertical sections

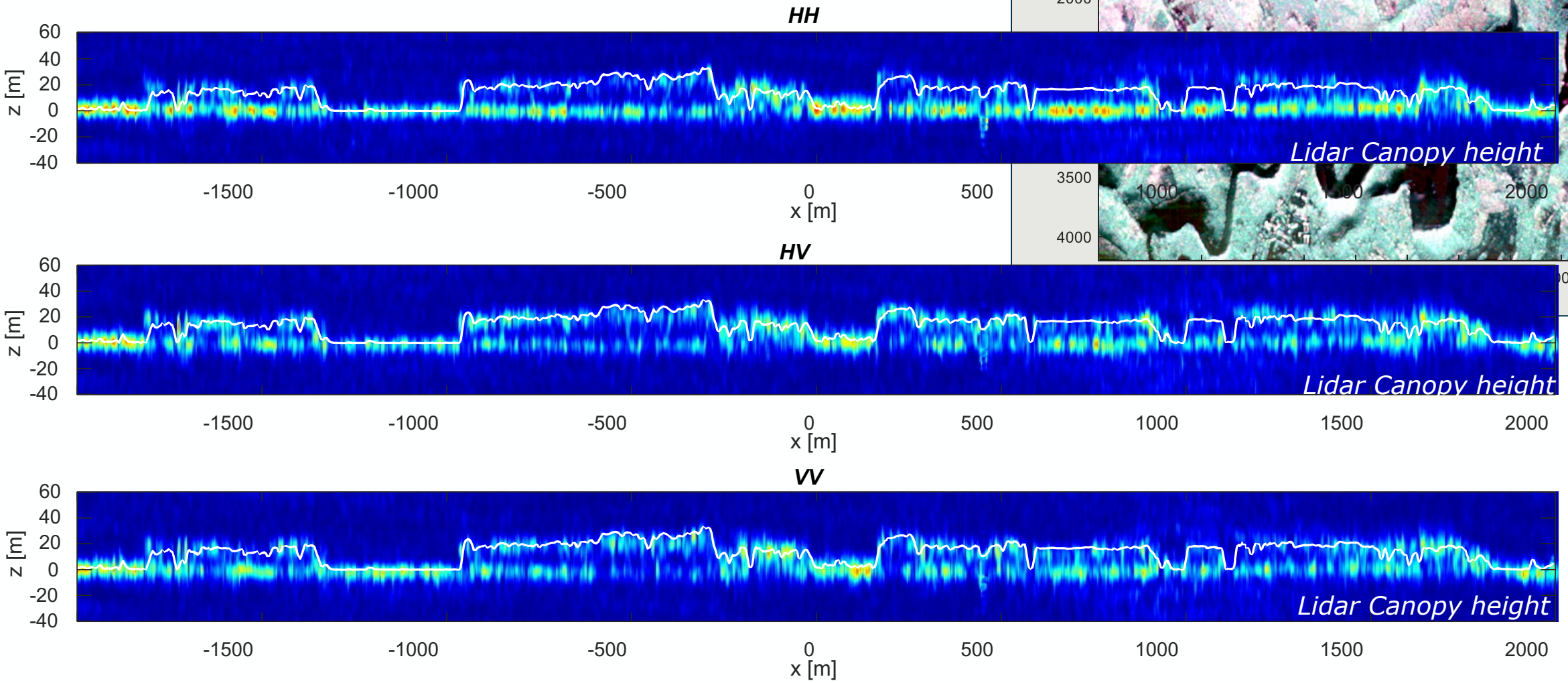

L-Band Tomography

Ground-steered L-Band vertical sections

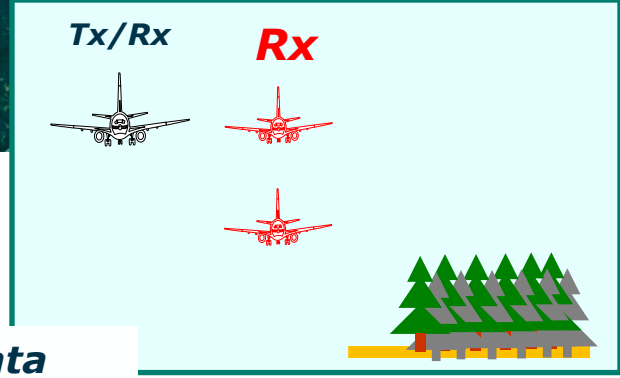

L-Band – HH – Vertical section from repeat pass mono-static data

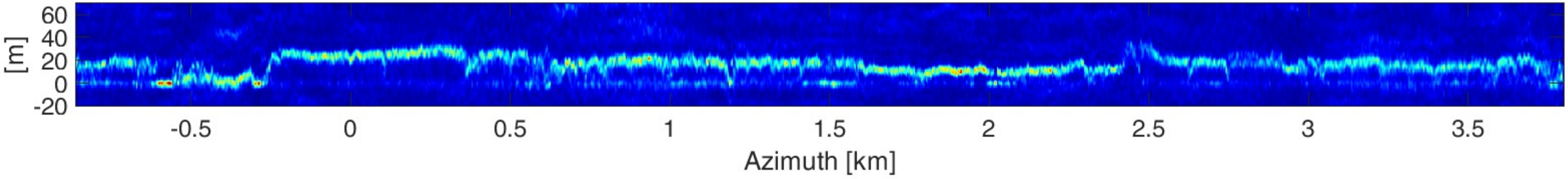

L-Band – HH – Vertical section from repeat pass bi-static data

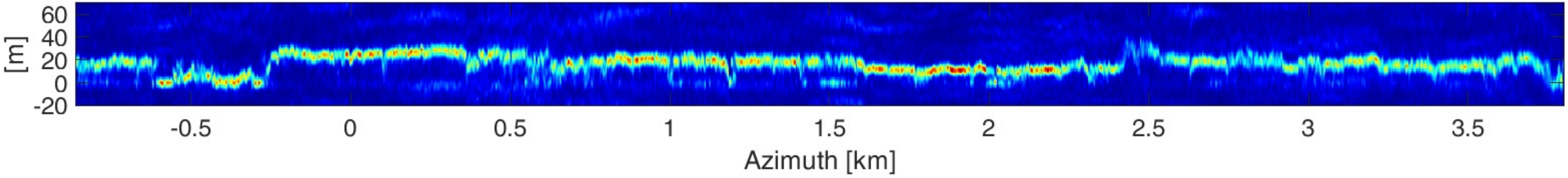

L-Band – HH – Vertical section from simultaneous Tx/Rx interferograms

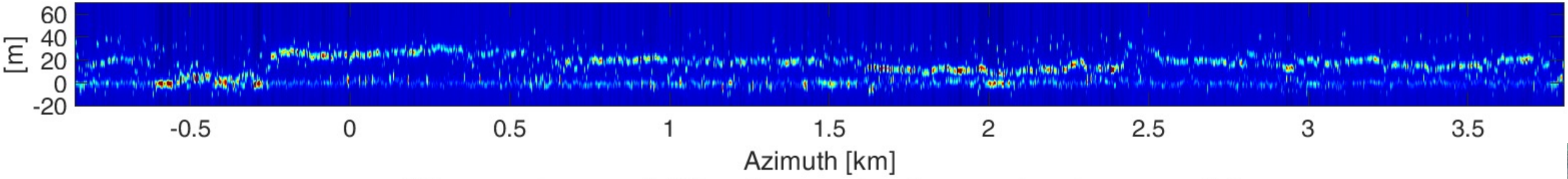

L-Band Tomography

Ground-steered L-Band vertical sections

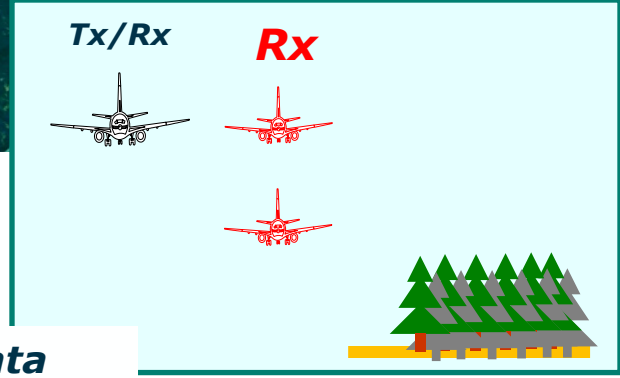

L-Band – HH – Vertical section from repeat pass mono-static data

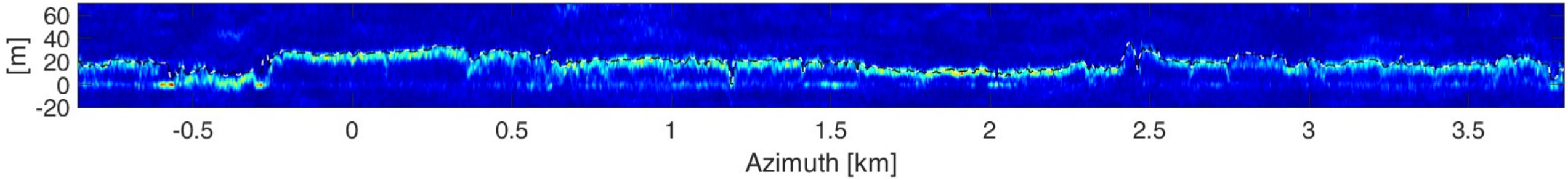

L-Band – HH – Vertical section from repeat pass bi-static data

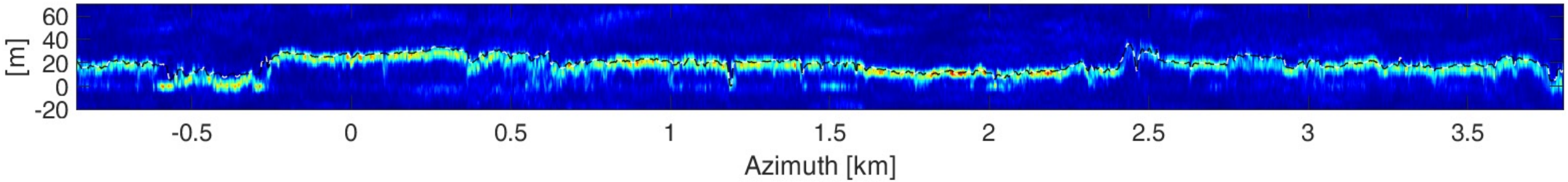

L-Band – HH – Vertical section from simultaneous Tx/Rx interferograms

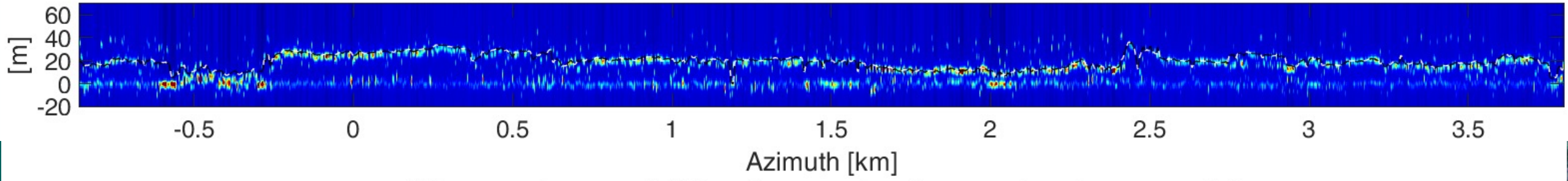

L-Band Tomography

Ground-steered L-Band vertical sections

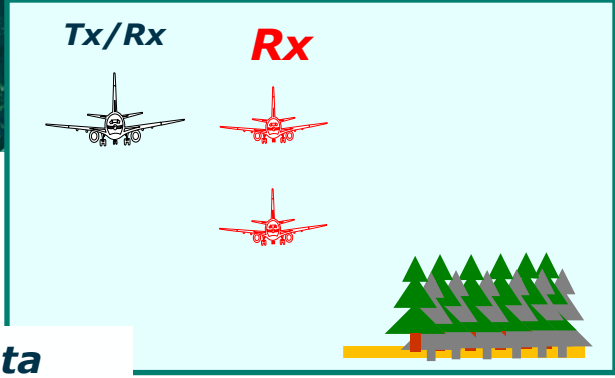

L-Band – HH – Vertical section from repeat pass mono-static data

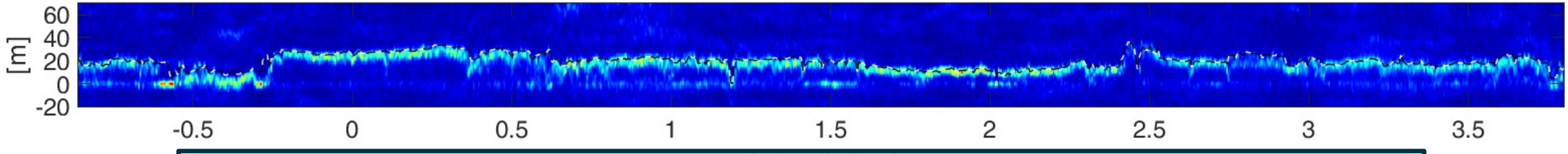

- Monostatic data gather more power from the ground w.r.t. bistatic
- Consistent with presence of ground-trunk double bounce scattering
- Almost same tomograms can be obtained with coherent pairs rather than a fully coherent stack of images, despite across-track baselines turned out to be significantly larger than planned due to a misinterpretation about the flight formation

L-Band – HH – Vertical section from simultaneous Tx/Rx interferograms

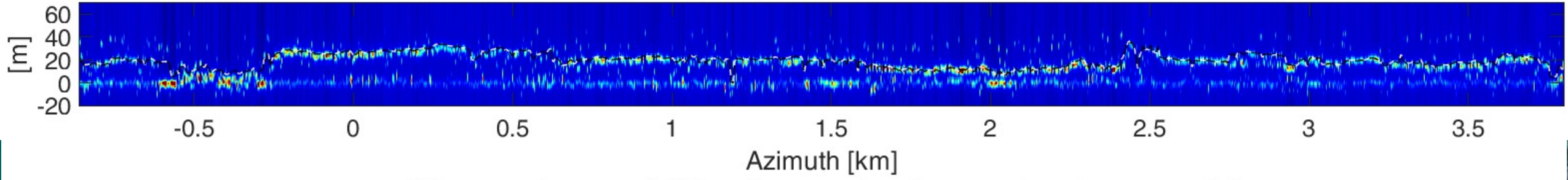

L-Band Tomography

Forest height retrieval from simultaneous L-Band Tx/Rx interferograms

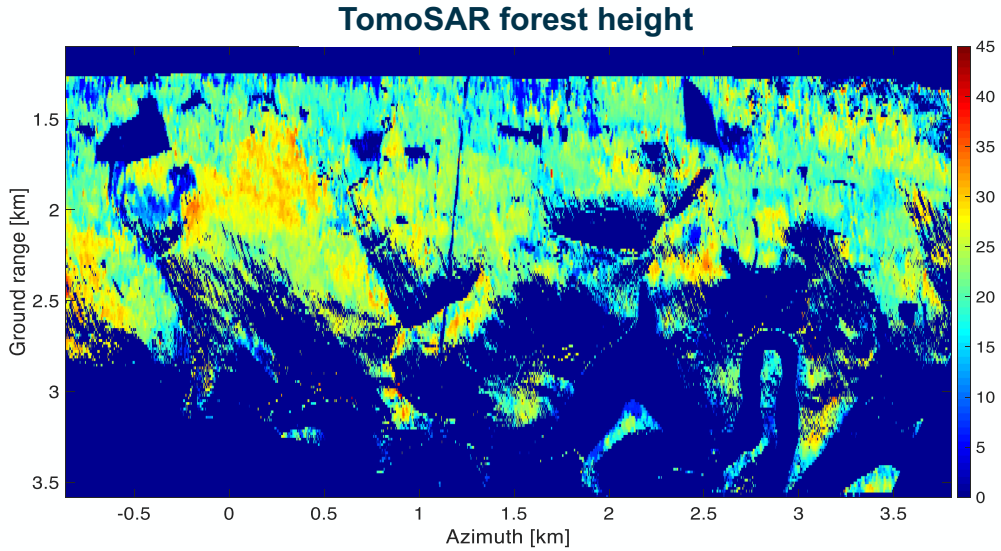

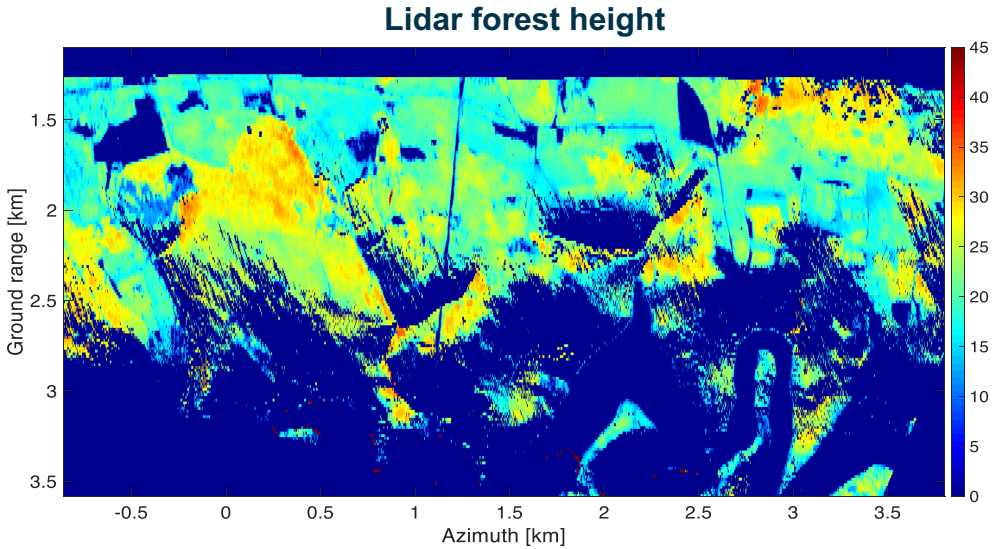

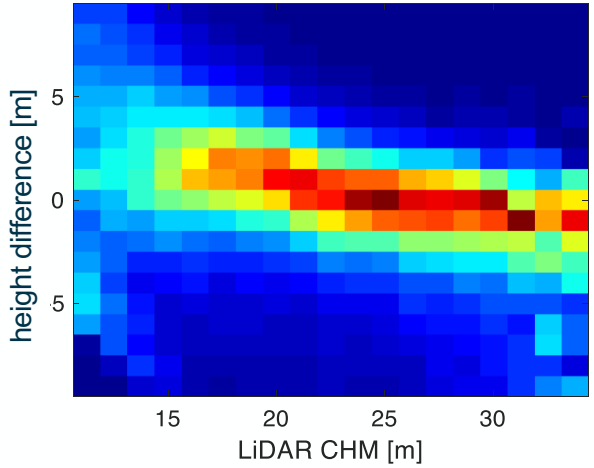

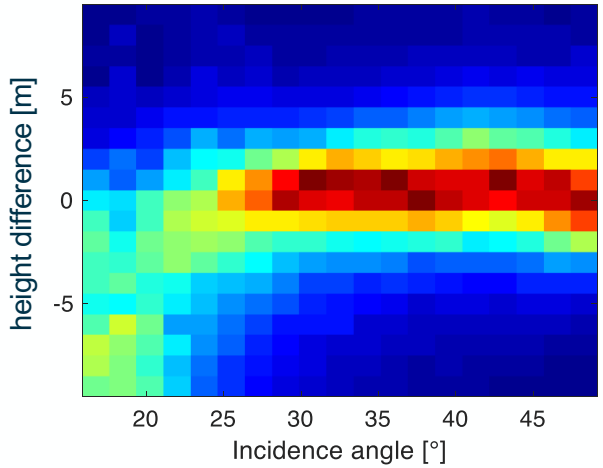

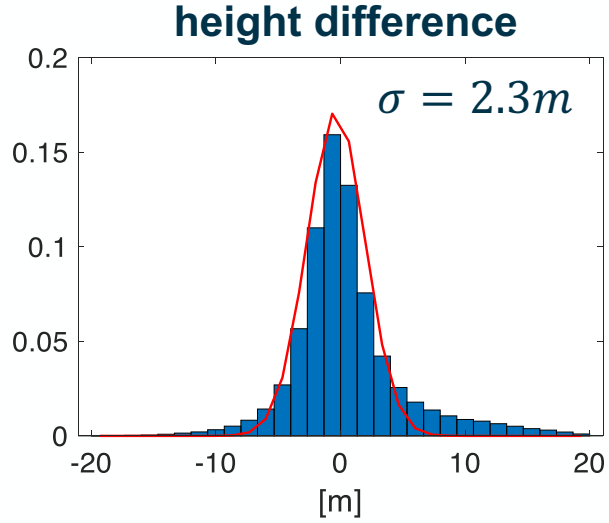

Ground-to-Volume Ratio in mono-static L-Band repeat-pass data

POLITECNICO MILANO 1863

Backscattered power cube:

- Gaussian filter $10m \times 12m \times 6m$ along x, y, and z
- Ground power P_{ground}: integrating $\pm 7m$ around DTM level
- Volume power P_{volume}: integrating $\pm 7m$ around DTM + CHM level

$$G2V(pol) = 10 \cdot log_{10} \frac{P_{ground}(pol)}{P_{volume}(pol)}$$

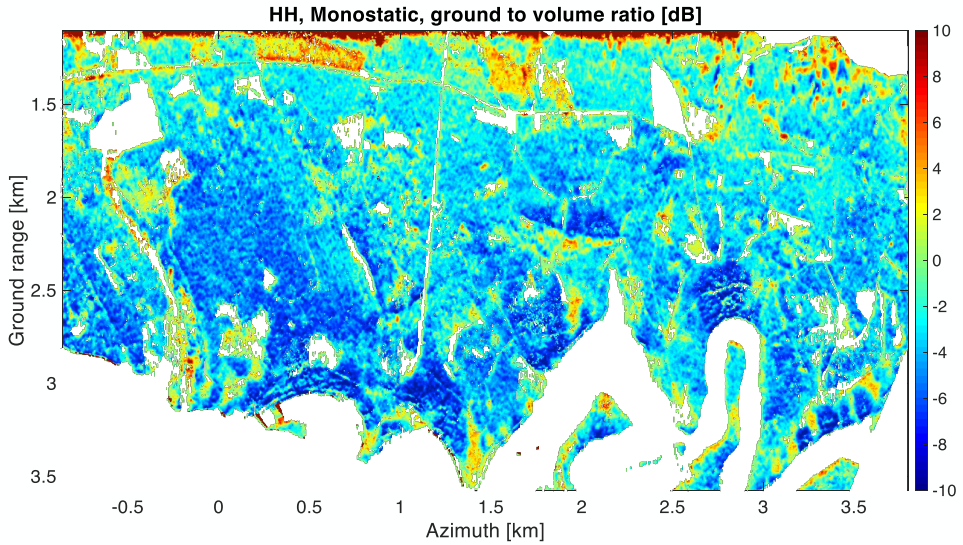

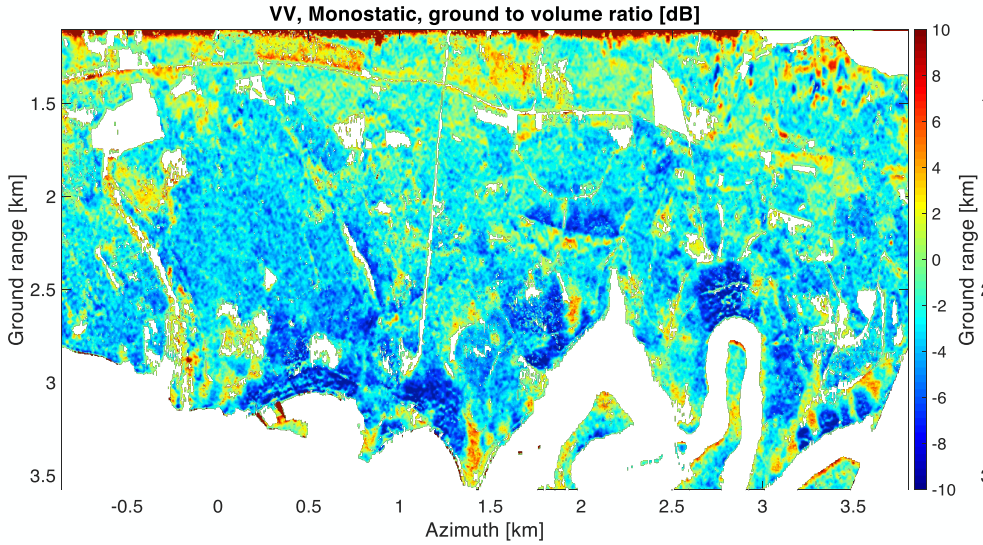

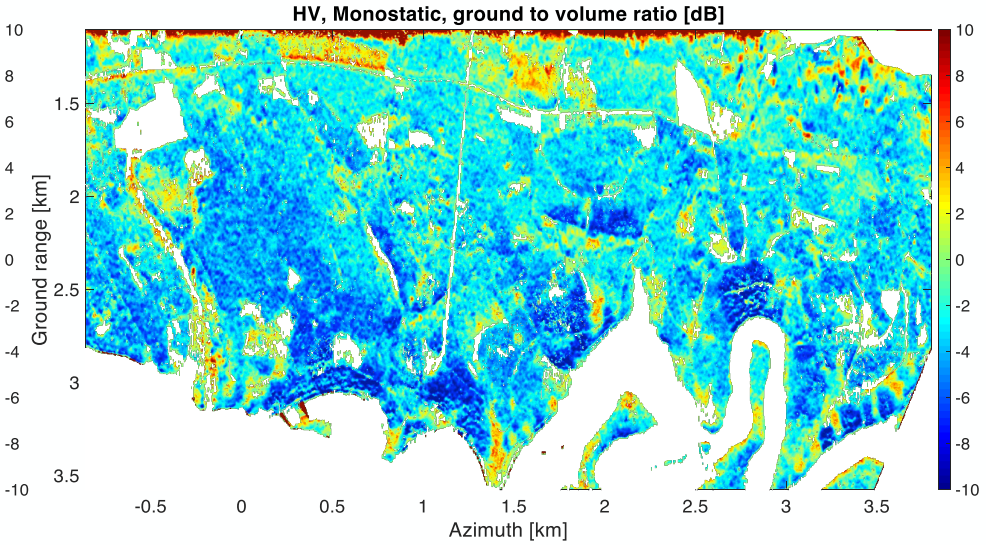

Ground-to-Volume Ratio in bi-static L-Band repeat-pass data

Backscattered power cube:

- Gaussian filter $10m \times 12m \times 6m$ along x, y, and z
- Ground power P_{ground}: integrating $\pm 7m$ around DTM level
- Volume power P_{volume}: integrating $\pm 7m$ around DTM + CHM level

$$G2V(pol) = 10 \cdot log_{10} \frac{P_{ground}(pol)}{P_{volume}(pol)}$$

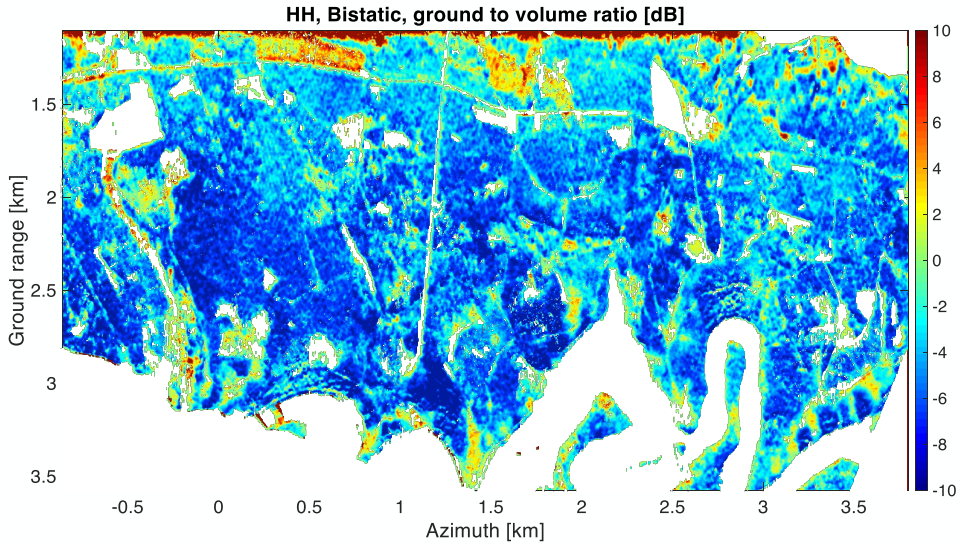

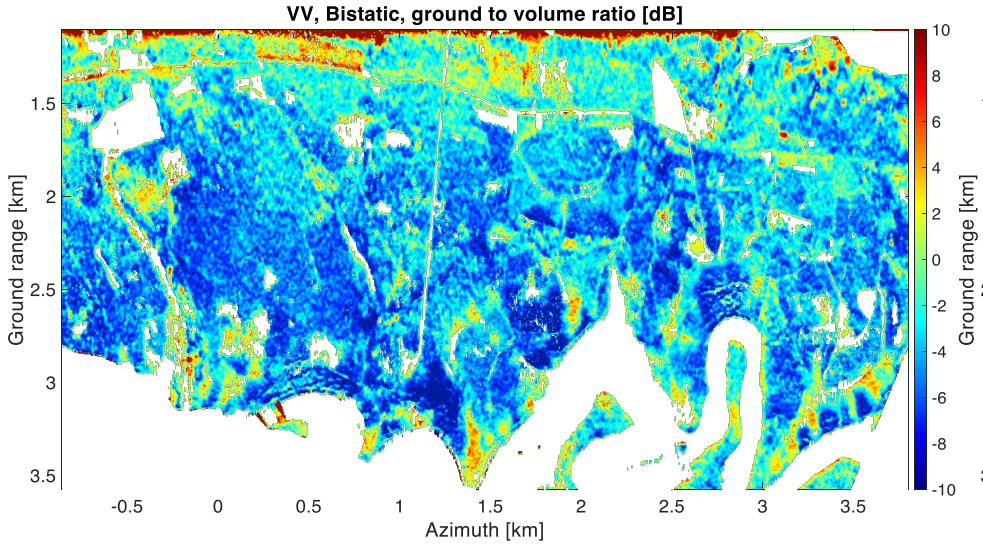

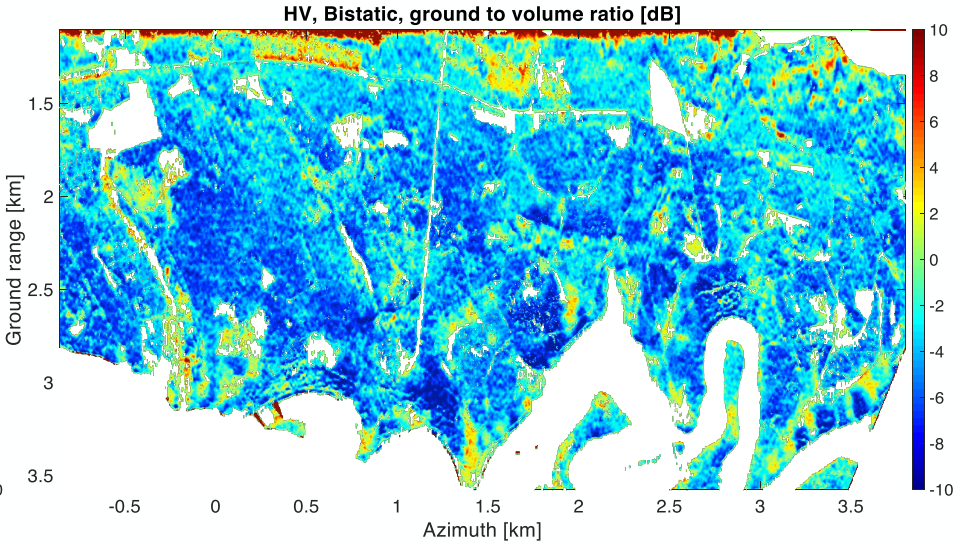

Ground-to-Volume Ratio in bi-static L-Band repeat-pass data

Backscattered power cube:

- Gaussian filter $10m \times 12m \times 6m$ along x, y, and z
- Ground power P_{ground}: integrating $\pm 7m$ around DTM level
- Volume power P_{volume}: integrating $\pm 7m$ around DTM + CHM level

$$G2V(pol) = 10 \cdot log_{10}\left(\frac{P_{ground}(pol)}{P_{volume}(pol)}\right)$$

- Lower ground-to-volume ratio with bistatic data
- Less power from the ground than monostatic
  - Might be due to ground-trunk double bounce
  - About 4dB less for bistatic data

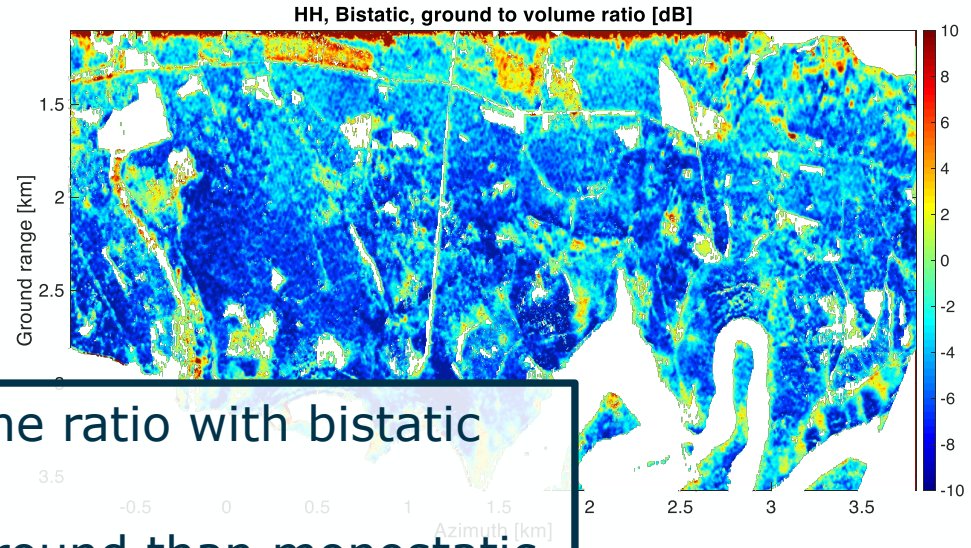

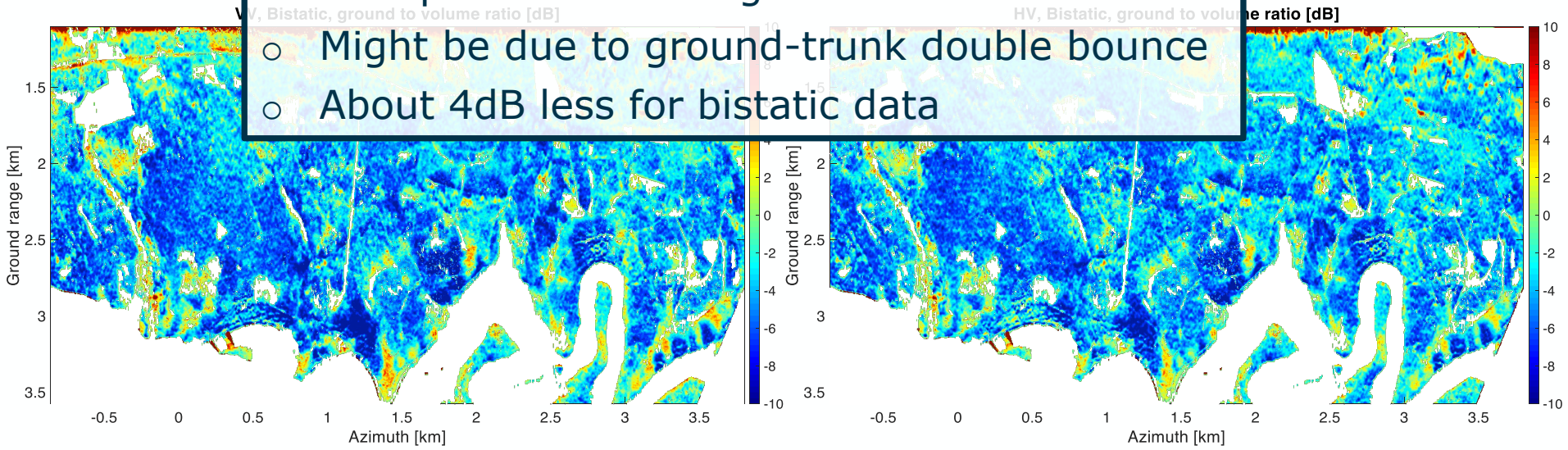

Ground-to-Volume Ratio in simultaneous L-Band pairs

Backscattered power cube:

- Gaussian filter $10m \times 12m \times 6m$ along x, y, and z
- Ground power P_{ground}: integrating $\pm 7m$ around DTM level
- Volume power P_{volume}: integrating $\pm 7m$ around DTM + CHM level

$$G2V(pol) = 10 \cdot log_{10} \frac{P_{ground}(pol)}{P_{volume}(pol)}$$

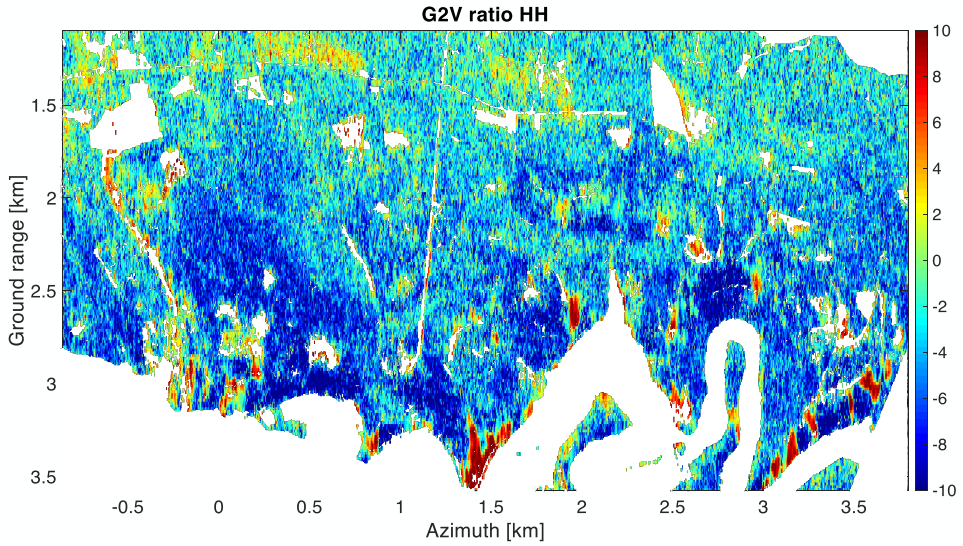

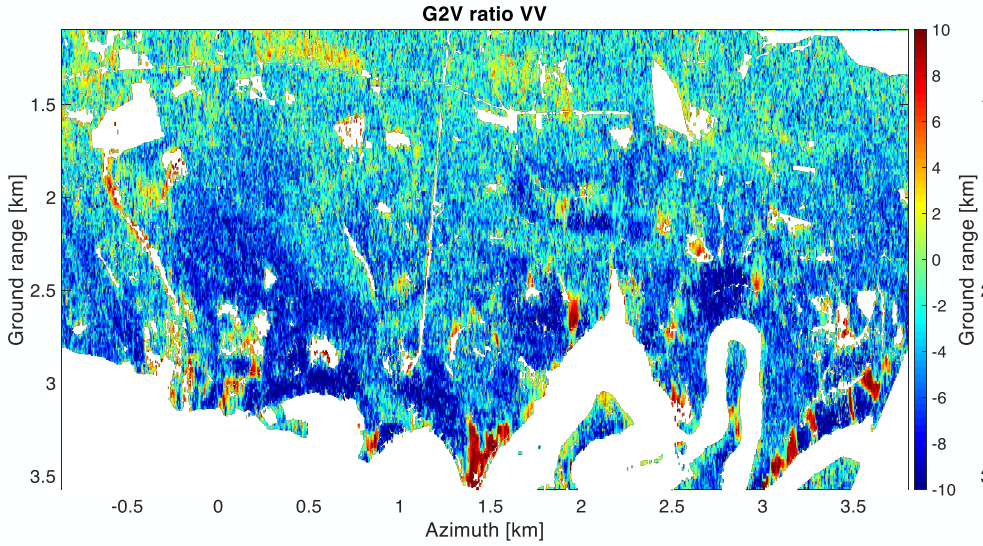

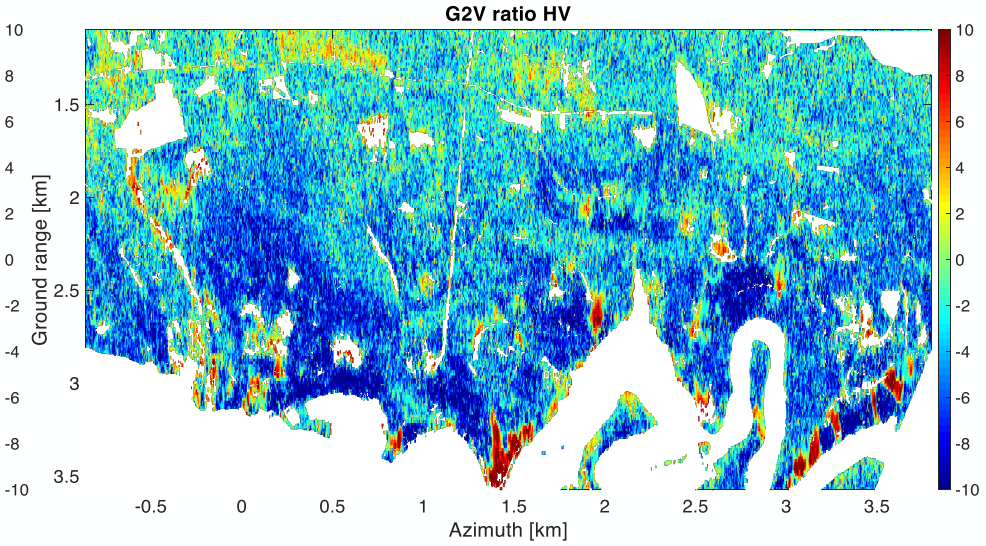

Ground-to-Volume Ratio in simultaneous L-Band pairs

Backscattered power cube:

- Gaussian filter $10m \times 12m \times 6m$ along x, y, and z
- Ground power P_{ground}: integrating $\pm 7m$ around DTM level
- Volume power P_{volume}: integrating around DTM + CHM level

$$G2V(pol) = 10 \cdot log_{10} \frac{P_{ground}(pol)}{P_{volume}(pol)}$$

- Same biophysical quantity estimated with coherent mono-bistatic pairs only
- Order of magnitude in complete agreement with standard repeat-pass estimates
- Quantitatively it appears in the middle between purely monostatic and purely bistatic G2V

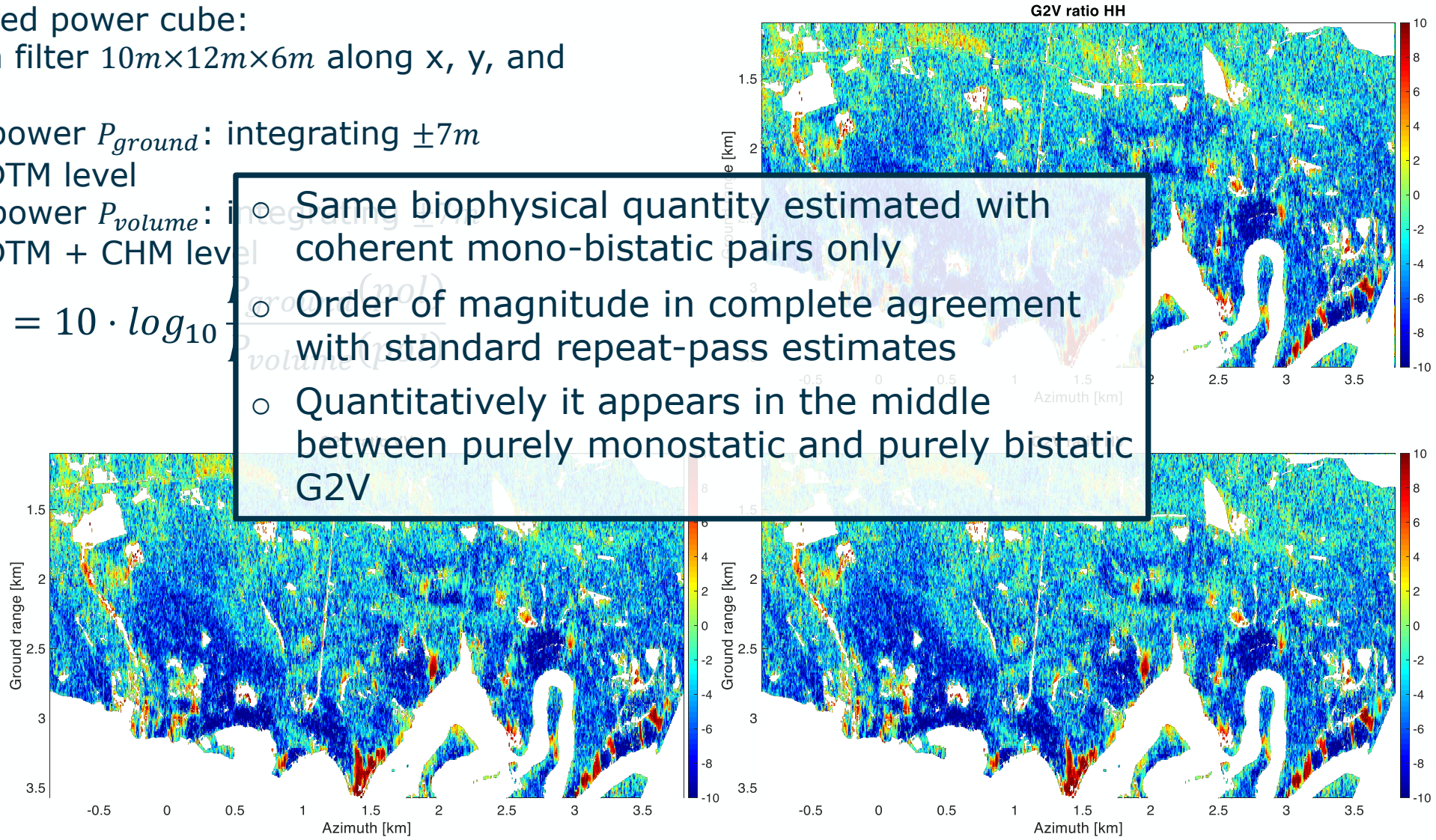

Overview of the results – sensitivity to AGB

Cross-validation between new AGB generated with TLS-derived allometry and SAR Tomography

AGB by Czechglobe with allometry from literature

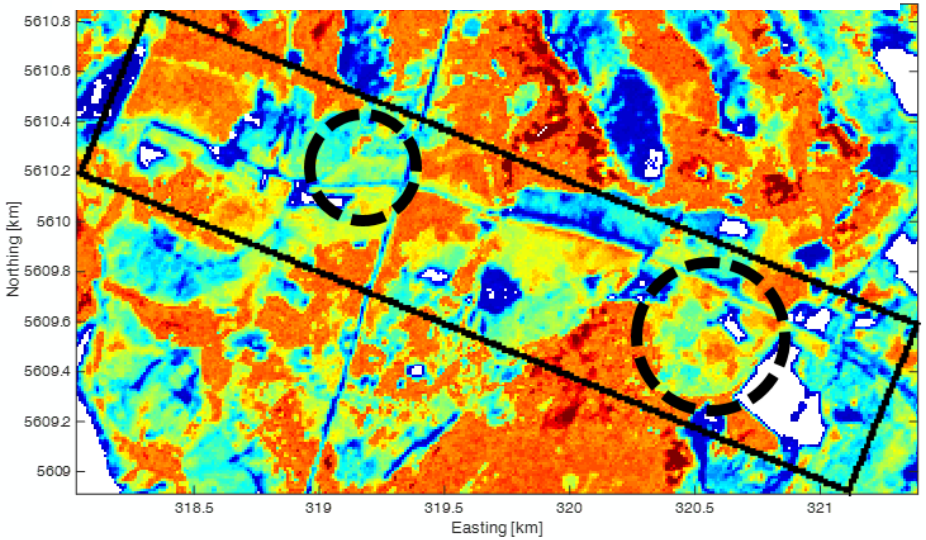

AGB by Czechglobe with allometry derived by UCL from TLS

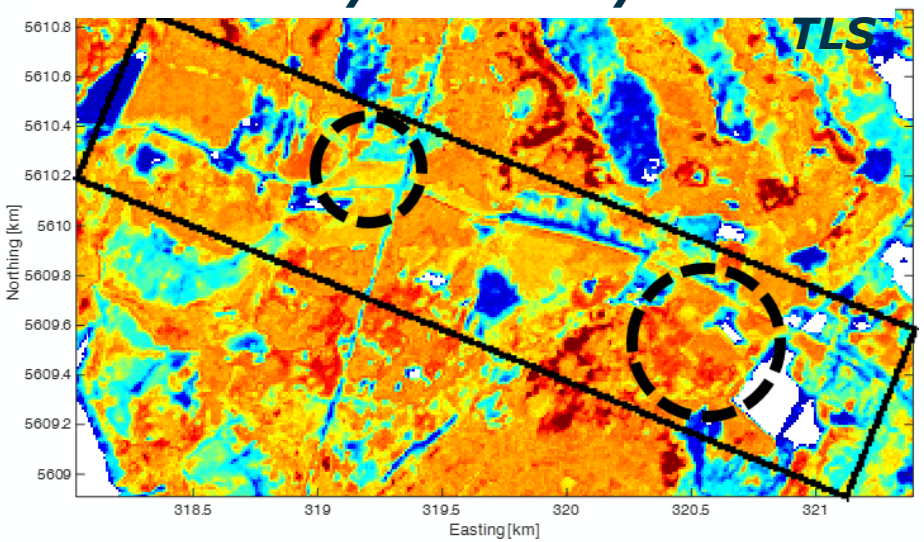

Canopy height

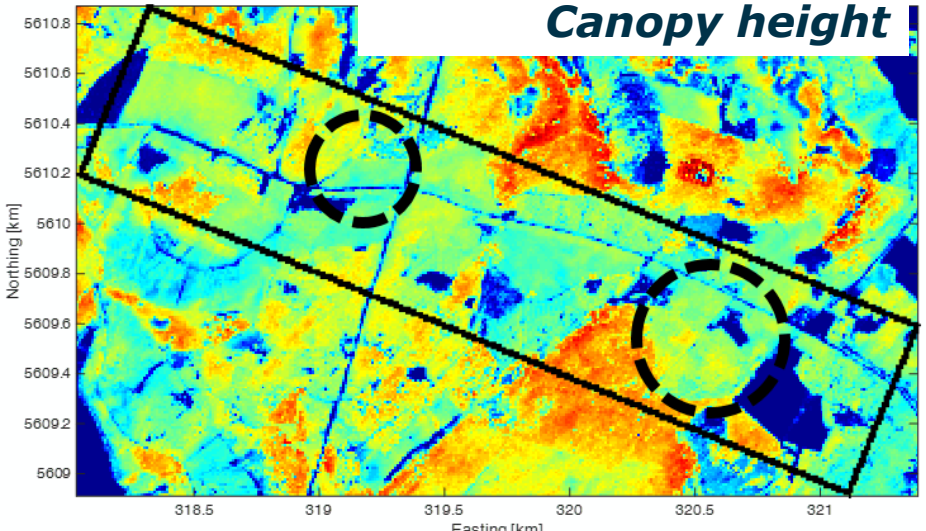

L-Band Volume-to-Ground Power Ratio

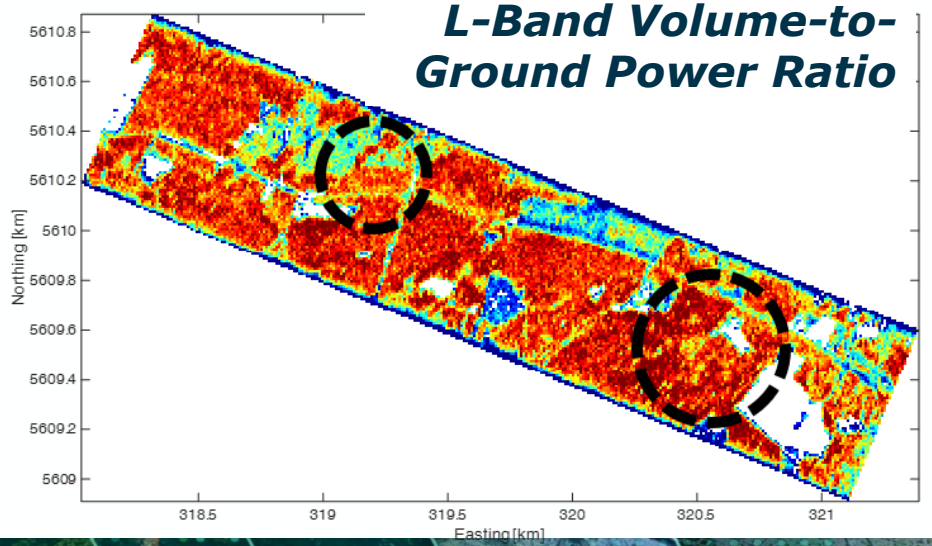

Overview of the results – comparison w.r.t. TLS

Comparison against bi-static L-Band tomography and TLS data acquired by University College London and Wageningen University in September 2021

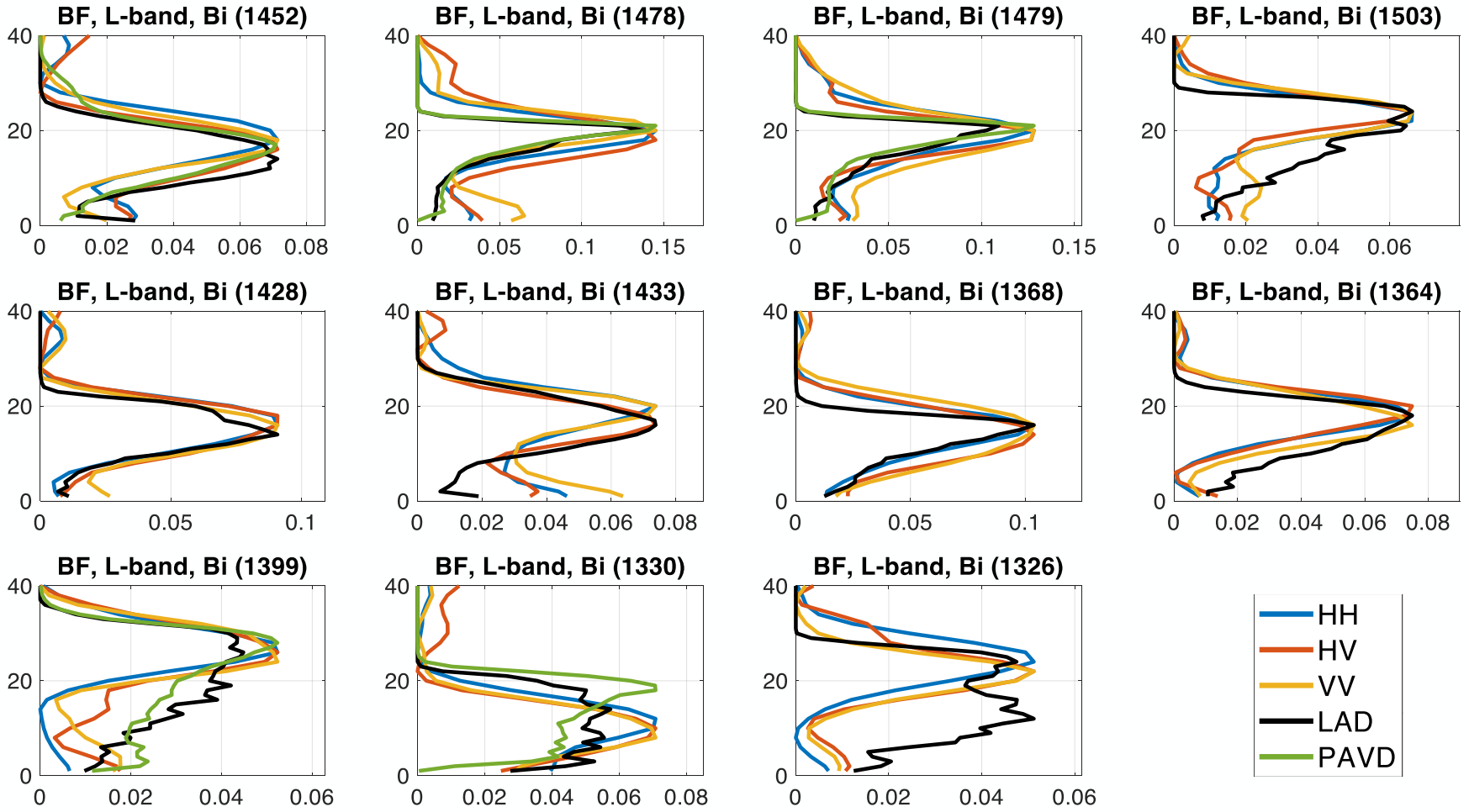

C-Band Tomography

Ground-steered C-Band vertical sections

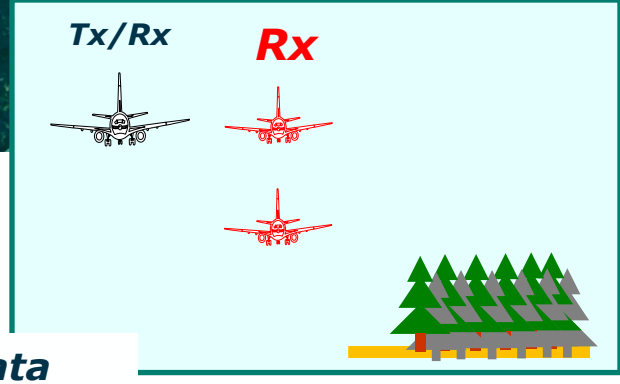

C-Band – HH – Vertical section from repeat pass mono-static data

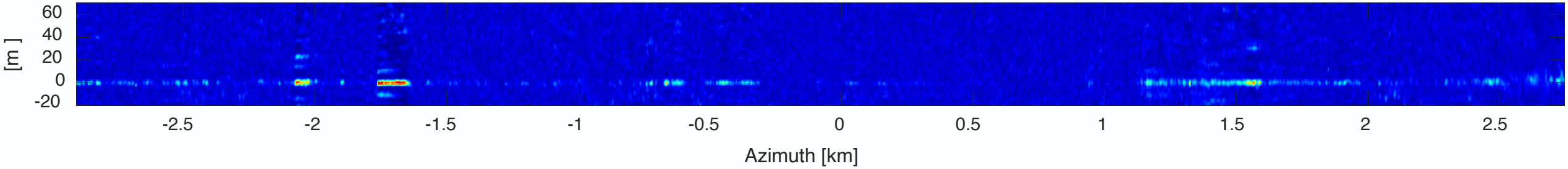

C-Band – HH – Vertical section from repeat pass bi-static data

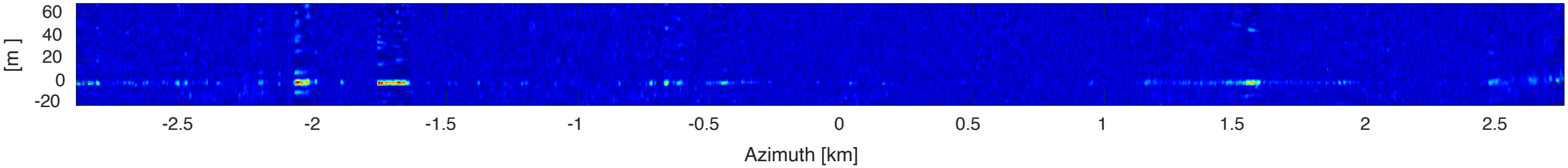

C-Band – HH – Vertical section from simultaneous Tx/Rx interferograms

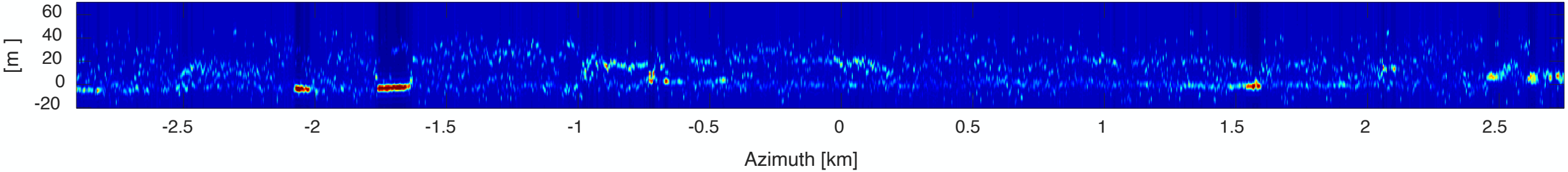

C-Band Tomography

Ground-steered C-Band vertical sections

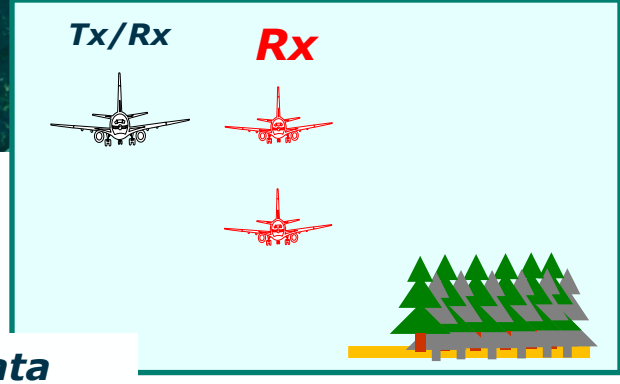

C-Band – HH – Vertical section from repeat pass mono-static data

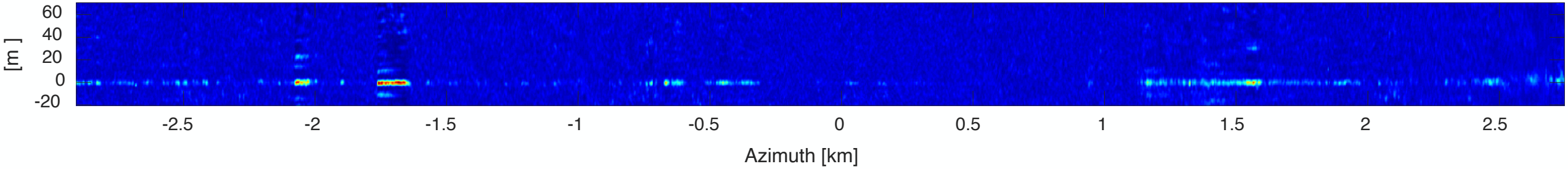

C-Band – HH – Vertical section from repeat pass bi-static data

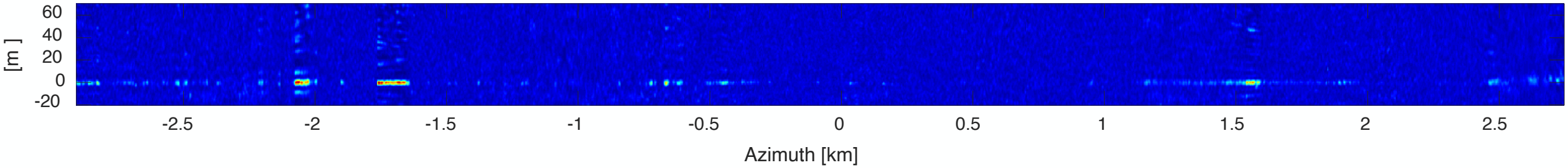

C-Band – HH – Vertical section from simultaneous Tx/Rx interferograms

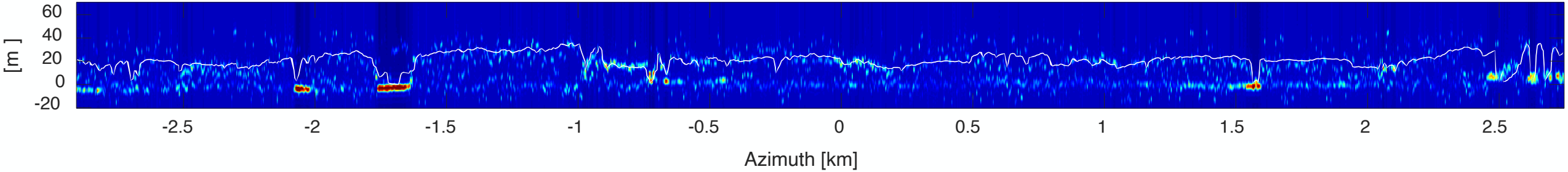

C-Band Tomography

Ground-steered C-Band vertical sections

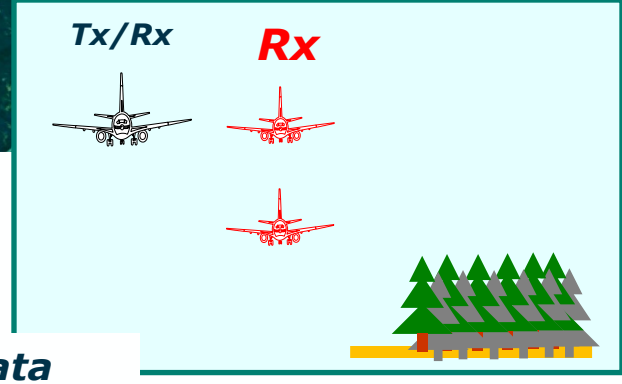

C-Band – HH – Vertical section from repeat pass mono-static data

- Ground is visible at C-band too below temperate forests (!)
- Correlation after 10 minutes is due to ground only
- 1 second is enough to decorrelate canopies but they are still visible
- Simultaneous image pairs were acquired with correct across-track baselines
- Yet, the along-track baseline couldn't be as small as planned due to safety reasons, causing a residual temporal decorrelation in simultaneous image pairs as well

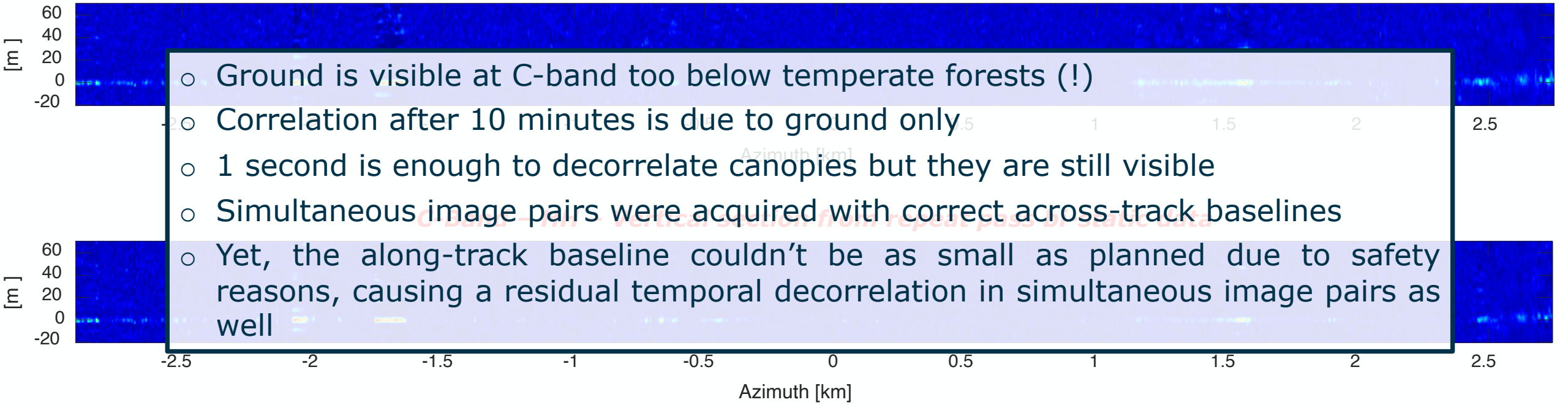

C-Band – HH – Vertical section from simultaneous Tx/Rx interferograms

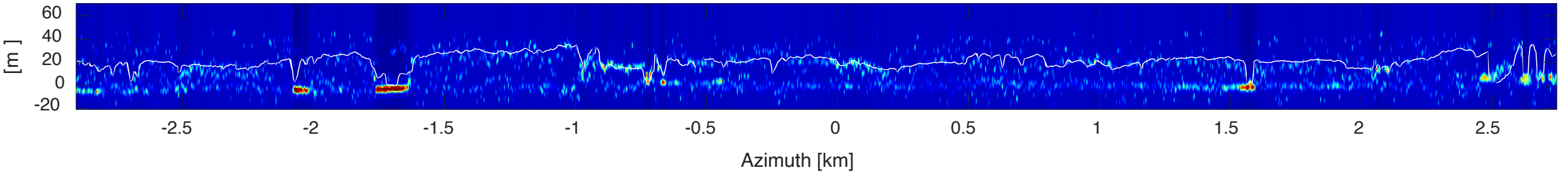

C-Band short-time temporal decorrelation

C-Band was re-flown to guarantee short across-track baselines. Yet, for safety reasons it was impossible to fly the two airplanes at the planned along-track distance of 20 m, resulting in a larger than expected effective delay between monostatic and bistatic acquisitions in the same overpass (say from 400 ms to 1 s instead of the planned value of 200 ms)

Planned formation

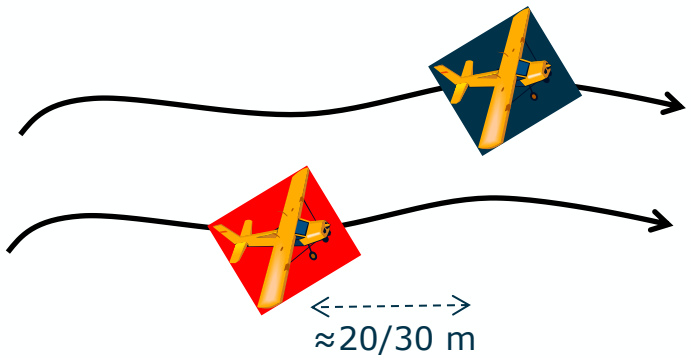

Actual formation

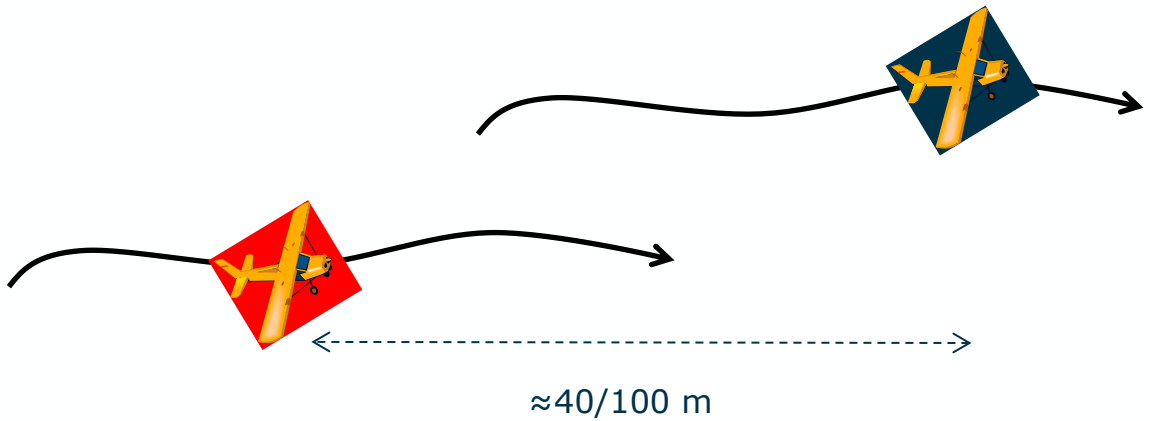

Not quite as planned, but we took the opportunity to study short-time temporal decorrelation at C-Band

C-Band short-time temporal decorrelation

Mono-bistatic coherence at C-Band (HH) for zero spatial across-track baseline

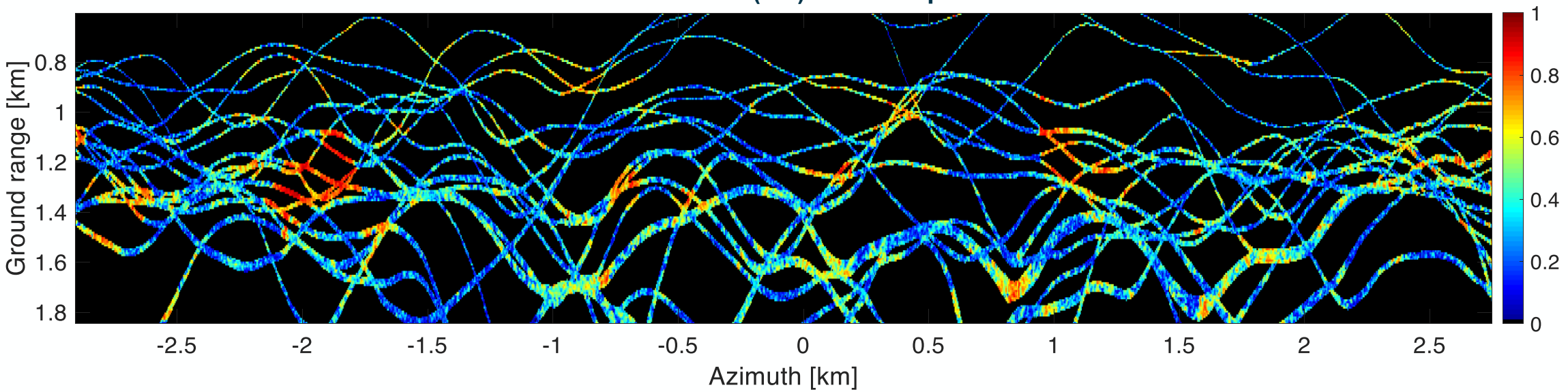

Remark:

- Very clear trend w.r.t. forest height and AGB

Zero spatial baseline

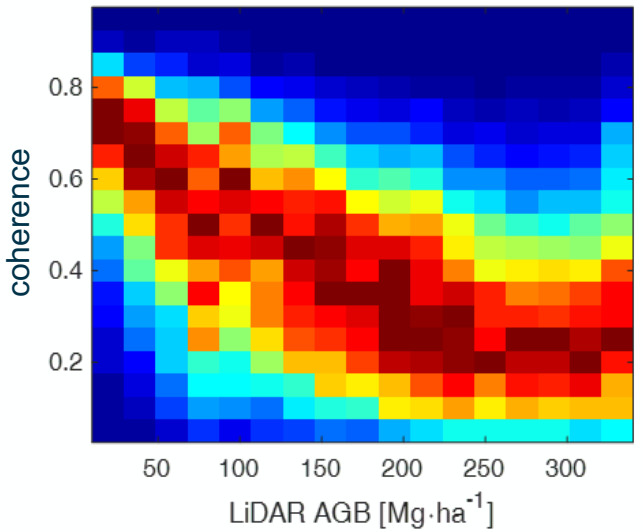

Zero spatial baseline

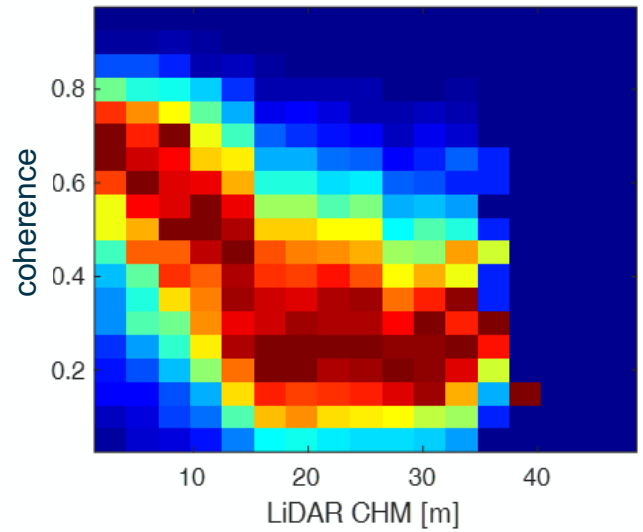

C-Band short-time temporal decorrelation

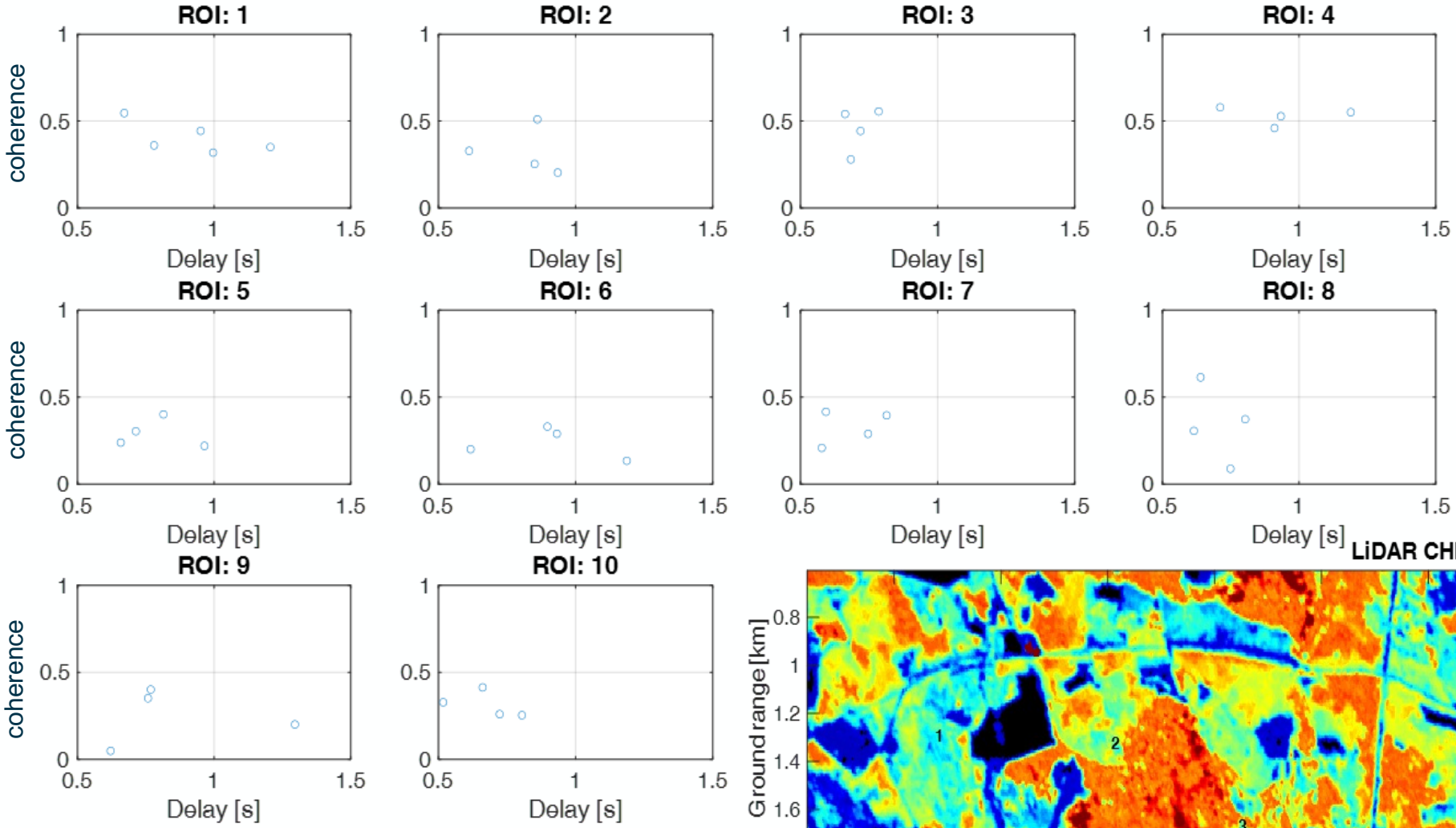

Specific locations explored at zero XT baseline in different overpasses

Remark:

- No clear trend, so much likely wind dependent

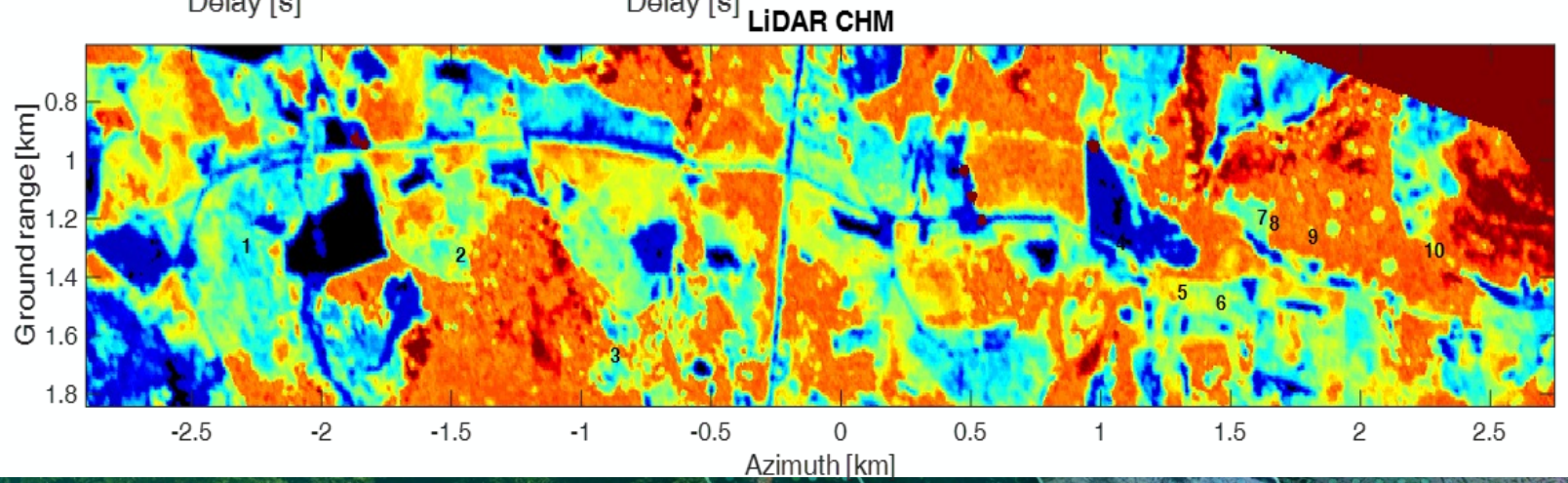

Discussion

P- and L-Band

Both P-and L-Band allow for a clear detection of terrain and forest canopies.

Sensitivity to forest AGB (see talk *TomoSAR Sensitivity to Temperate Forest Above-Ground Biomass at P- and L-band in the TomoSense ESA Campaign*)

Bistatic data exhibit lower contributions from the ground level, resulting in the GVR to be lower by about 4 dB

Correlation tomography using simultaneous Tx/Rx interferograms is observed to provide consistent results w.r.t. conventional repeat-pass approaches

C-Band

The residual coherence in repeat-pass interferograms is mostly determined by scattering from the ground level, whereas the signal from the forest canopy is nearly impossible to detect because of temporal decorrelation.

Results indicate that C-Band waves care capable of penetrating down to the ground level.

This finding provides an element in support of the feasibility of C-Band tomography of temperate forests, clearly provided that acquisitions are taken at a temporal baselines of a few tens of milliseconds at most.

The TomoSense data-set

The TomoSense data-set is intended to serve as an important basis for studies on microwave scattering from forested areas in the context of future studies on Earth Observation missions.

The data-set includes:

- Calibrated SAR images and tomographic cubes at different levels of processing
- ALS-derived maps of forest height and AGB
- Forest census
- TLS profiles.

Complex SAR images are already finely coregistered, phase calibrated, and ground steered, in such a way as to enable future researchers to directly implement any kind of interferometric or tomographic processing without having to deal with the subtleties of airborne SAR data.

In addition to that, the data-base comprises tomographic cubes representing forest scattering in 3D both in Radar and geographical coordinates, which are intended for use by non-Radar experts.

The TomoSense data-set

The TomoSense data-set is intended to serve as an important basis for studies on microwave scattering from forested areas in the context of future studies on Earth Observation missions.

The data-set includes:

- Calibrated SAR images and tomographic cubes at different levels of processing
- ALS-derived maps of forest height and AGB
- Forest census
- TLS profiles.

The whole data-set is freely available for any research purpose

- Through ESA's portal (will come)
- By sending me an email at:

stefano.tebaldini@polimi.it

(*I'll reply with a DropBox link*)

Complex SAR images are already fine-tuned to the ground steered, in such a way as to enable future researchers to directly implement any kind of interferometric or tomographic processing without having to deal with the subtleties of airborne SAR data.

In addition to that, the data-base comprises tomographic cubes representing forest scattering in 3D both in Radar and geographical coordinates, which are intended for use by non-Radar experts.